A rapid and efficient screening system for neutralizing antibodies and its application for SARS-CoV-2

Xiaojian Han
Chongqing Medical University
Yingming Wang
Chongqing Medical University
Shenglong Li
Chongqing Medical University
Chao Hu
Institute for Infectious Diseases and Vaccine Development, Tongji University School of Medicine
Tingting Li
Chongqing Medical University
Chenjian Gu
Fudan University
Kai Wang
Key Laboratory of Molecular Biology on Infectious Diseases, Ministry of Education, Chongqing Medical University https://orcid.org/0000-0002-0137-1247
Meiying Shen
Harbin Medical University
Jianwei Wang
Chongqing Medical University
Jie Hu
Chongqing Medical University
Ruixin Wu
Chongqing Medical University
Song Mu
Chongqing Medical University
Fang Gong
Chongqing Medical University
Qian Chen
Chongqing Medical University
Fengxia Gao
Chongqing Medical University

Jingjing Huang
Chongqing Medical University
Yingyi Long
Chongqing Medical University
Feiyang Luo
Chongqing Medical University
Shuyi Song
Chongqing Medical University
Shunhua Long
Chongqing Medical University
Yanan Hao
Chongqing Medical University
Luo Li
Chongqing Medical University
Yang Wu
Fudan University
Wei Xu
Shanghai Medical College, Fudan University
Xia Cai
Fudan University
Qingzhu Gao
Chongqing Medical University
Guiji Zhang
Chongqing Medical University
Changlong He
The First Affiliated Hospital of Chongqing Medical University
Kun Deng
Chongqing Medical University
Li Du
Chongqing Medical University
Yaru Nai
Chongqing Medical University
Wang Wang
Chongqing Medical University
Youhua Xie
Fudan University
Di Qu
Fudan University
Ailong Huang

Chongqing Medical University https://orcid.org/0000-0003-0148-7423

Ni Tang

Chongqing Medical University https://orcid.org/0000-0001-5830-8786

Aishun Jin (aishunjin@cqmu.edu.cn)

Chongqing Medical University

Article

Keywords: SARS-CoV-2, neutralizing antibodies, methodology, spike protein, receptor-binding domain

Posted Date: October 28th, 2020

DOI: https://doi.org/10.21203/rs.3.rs-87599/v1

Version of Record: A version of this preprint was published at Frontiers in Immunology on March 22nd, 2021. See the published version at https://doi.org/10.3389/fimmu.2021.653189.

A rapid and efficient screening system for neutralizing antibodies and its application for SARS-CoV-2

Xiaojian Han[1,2,8], Yingming Wang[1,2,8], Shenglong Li[1,2,8], Chao Hu[1,2], Tingting Li[1,2], Chenjian Gu[3], Kai Wang [4], Meiying Shen[5], Jianwei Wang[1,2], Jie Hu[4], Ruixin Wu[1,2], Song Mu[1,2], Fang Gong[6], Qian Chen[1,2], Fengxia Gao[1,2], Jingjing Huang[1,2], Yingyi Long[1,2], Feiyang Luo[1,2], Shuyi Song[1,2], Shunhua Long[1,2], Yanan Hao[1,2], Luo Li[1,2], Yang Wu[3], Wei Xu[3], Xia Cai[3], Qingzhu Gao[4], Guiji Zhang[4], Changlong He[4], Kun Deng[7], Li Du[1,2], Yaru Nai[1,2], Wang Wang[1,2], Youhua Xie[3], Di Qu[3], Ailong Huang[4], Ni Tang[4*] and Aishun Jin[1,2*]

[1]Department of Immunology, College of Basic Medicine, Chongqing Medical University, No.1 Yixueyuan Road, Yuzhong District, Chongqing 400016, P.R.China

[2]Chongqing Key Laboratory of Basic and Translational Research of Tumor Immunology, Chongqing Medical University, No.1 Yixueyuan Road, Yuzhong District, Chongqing 400016, P.R.China

[3]Key Laboratory of Medical Molecular Virology, Department of Medical Microbiology and Parasitology, School of Basic Medical Sciences, Shanghai Medical College, Fudan University, No.130 Dongan Road, Xuhui District, Shanghai 200433, P.R.China.

[4]Key Laboratory of Molecular Biology on Infectious Diseases, Ministry of Education, Chongqing Medical University, No.1 Yixueyuan Road, Yuzhong District, Chongqing 400016, P.R.China

[5]Department of Breast Surgery, Harbin Medical University Cancer Hospital, No.150 Haping Road, Nangang District, Harbin 150081, Heilongjiang Province, P.R.China

[6]Department of Pediatrics, Yongchuan Hospital Affiliated to Chongqing Medical University, No.439 Xuanhua Road, Yongchuan District, Chongqing 402160, P.R.China

[7]Department of laboratory, The Third Affiliated Hospital of Chongqing Medical University, No.1 Shuanghu Road, Yubei District, Chongqing 401120, P.R.China

[8]These authors contributed equally to this work.

[*]Correspondence: aishunjin@cqmu.edu.cn (A.S.J); nitang@cqmu.edu.cn (N.T.).

Keywords: SARS-CoV-2, neutralizing antibodies, methodology, spike protein, receptor-binding domain

Abstract

After the epidemic of COVID-19, neutralizing antibodies (NAbs) against SARS-CoV-2 has been developed for the preventative and therapeutic purposes. However, few methodologies are reported in detail on how to rapidly and efficiently generate NAbs of interest. Here, we present a strategically optimized screening method for NAbs, which has enabled us to obtain SARS-CoV-2 receptor-binding domain (RBD) specific monoclonal Abs within 4 days, followed by additional 2 days to evaluate their neutralizing activities. Using this method, we obtained 198 specific Abs against SARS-CoV-2 RBD from the blood samples of COVID-19 convalescent patients, and 96 of them showed neutralizing activity. At least 20% of these NAbs exhibited high neutralizing potency. The top 2 NAbs showed the half-maximal inhibitory concentration (IC_{50}) to block authentic SARS-CoV-2 at 9.88 and 11.13 ng/ml, respectively. Altogether, our study provides a fundamental methodology for discovering NAbs with potential preventative and therapeutic value for emerging infectious diseases.

Introduction

In the past two decades, pandemic outbreaks of three novel pathogenic human coronaviruses, severe acute respiratory syndrome coronavirus 2 (SARS-CoV-2), Middle East respiratory syndrome coronavirus (MERS-CoV) and SARS-CoV, have caused high mortality and unprecedented social and economic consequences[1-4]. While vaccines are effective in blocking infectious diseases, NAbs are an alternative treatment strategy for preventing virus infection. During the outbreaks of SARS-CoV and MERS-CoV, convalescent patients' plasma containing NAbs was a safe and effective treatment option to reduce mortality in severe cases[5,6]. However, convalescent plasma is limited and the polyclonal non-neutralizing Abs in the plasma may cause undesired side effects[7]. The NAb therapeutics is an effective replacement of convalescent plasma therapy. Therefore, a rapid and efficient virus NAbs screening method is greatly needed.

The viral spike (S) of SARS-CoV-2 containing the receptor-binding domain (RBD) is responsible for binding to the receptor angiotensin-converting enzyme-2 (ACE2) receptor on the host cells[8,9]. To date, some potent NAbs to SARS-CoV-2 have been promptly developed by different teams, with various methodologies employed for the screening of NAbs[10-23]. Some studies utilized SARS-CoV-2 S- or RBD-labeled memory B cells from COVID-19 convalescent patients, and directly amplified Ab genes by RT-PCR and nested PCR at a single-cell level[17,21]. Others activated and expanded plasma cells with stimulators and cytokines *in vitro* to select NAbs[11,12]. Also, humanized mice were used to generate full human mAbs against S protein[10,23]. Furthermore, the single-cell sequencing technology was applied in combination with the enrichment of antigen-specific B cells, which led to the quick detection of thousands of antigen specific mAbs sequences[14,15]. Although these studies showed that NAbs against SASR-CoV-2 could be obtained from convalescence patients, few methodologies were reported in detail focusing on the rapid and efficient generation of NAbs of interest.

Here, we established a strategically optimized system for the fast screening of mAbs with neutralizing capability in, as short as, 6 days. A total of 198 Abs against RBD of SARS-CoV-2 were obtained with this method, and 50% of them were potential NAb candidates in a preliminary screening with SARS-CoV-2 pseudovirus. Furthermore, the top 2 NAbs exhibit IC_{50} of around 10 ng/mL against authentic SARS-CoV-2. Therefore, this screening system can efficiently generate a large number of potent NAbs, which facilitate the development of NAbs candidate biologics for treatment and prevention of SARS-CoV-2 infection.

Results

Establishment of a rapid and efficient NAbs screening system. We established an optimized screening system for NAbs, using antigen specific memory B cells from the PBMC of patients with infectious diseases (Fig. 1). At first, the blood samples were collected from COVID-19 convalescent patients. Antigen specific memory B cells (mB cells) in a pooled PBMC from 5-7 patients were detected by labeling with RBD of SARS-CoV-2 and sorted into 96-well plates in a single-cell manner. The variable region of immunoglobulin heavy chains (IGH) and light chains (IGK or IGL) were obtained by RT-PCR and nested PCR, with the optimized primers, at Day 1 (Supplementary Table 1). Recombinant sites were introduced during the second PCR. Next, linear expression cassettes were assembled by overlapping PCR[24], which contained the essential elements for Ab gene transcription, including the CMV promoter, the antibody variable region, the antibody constant region, and the poly(A)-tail (Supplementary Table 2). Then, HEK293T cells were transiently transfected with these linear expression cassettes at Day 2. Supernatants of the transfected cells were evaluated for the S and RBD specific binding activities by enzyme-linked immunosorbent assay (ELISA) at Day 4, and their neutralizing capacities to pseudovirus were tested at Day 6. Subsequently, potent neutralizing Abs were expressed and purified for the functional analyses, including antigen reactivity, viral neutralization, and binding affinity, all of which were completed within the next 9 days. Overall, with this screening system, it only takes 15 days to obtain high potent NAbs against SARS-CoV-2.

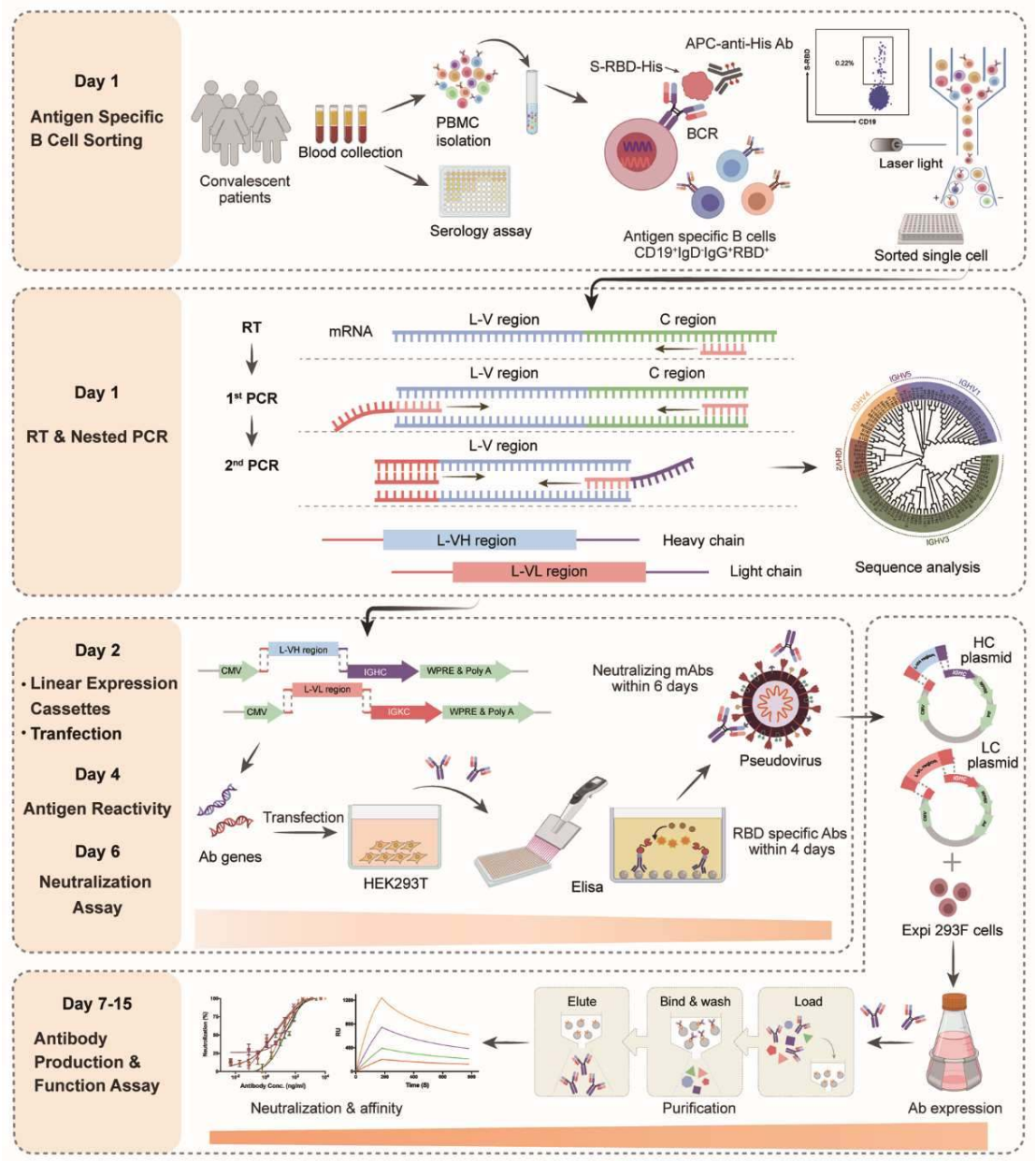

Fig. 1 Schematic overview of the rapid and efficient NAbs screening system. Rapid NAbs screening workflows and timelines are shown, representing the multiple processes conducted in order. The PBMC were isolated from collected convalescent patients' blood, and the RBD-specific memory B cells in the PBMC were sorted as single cells via flow cytometry (day 1). Then, the IgG heavy and light chains of mAb genes were amplified by RT-PCR on the same day. 2nd PCR products were cloned into the linear expression cassettes (day 2). HEK293T cells expressed antibodies by transient transfection with equal amounts of paired heavy and light chain linear expression cassettes and culture for 48 hours. The supernatants were used to detect the antigen reactivity of antibodies by ELISA in 384-well plates (day 4). The neutralizing activities of antibodies were measured with pseudovirus bearing SARS-CoV-2 S in 96-well plates (day 6). Plasmids expressing potential NAbs were transfected into Exi293F cells for the large-scale production of Ab proteins. The cell supernatants of Exi293F cells were collected, and the antibody proteins were purified by protein G beads. Antigen reactivity, neutralizing activity, and binding affinity were further accessed via ELISA, competitive ELISA, and surface plasmon resonance (SPR). *Figures were created with Biorender.com.*

Isolation of antibody genes from the single RBD-specific memory B cells. We collected the plasma of 39 COVID-19 convalescent patients admitted to Chongqing Medical University affiliated

106 Yongchuan Hospital (Supplementary Table 3). Such convalescent plasma had been preliminarily
107 screened and confirmed with the positive virus-specific binding and neutralizing capacities, using a
108 magnetic chemiluminescence enzyme immunoassay (MCLIA) and a pseudovirus-based assay[25]. We
109 confirmed that those Abs targeting Spike or the recombinant RBD of SARS-CoV-2, SARS-CoV, and
110 MERS-CoV in the plasma with 10-fold dilution, using ELISA assay. Among the 39 convalescent
111 plasma samples, 36 showed high reactivity to SARS-CoV-2 S or RBD proteins, while the other three
112 had weak responses (Fig. 2a). Almost all samples cross-reacted with the S1 protein of SARS-CoV or
113 that of MERS-CoV, with either 10-fold or 100-fold dilutions, while the healthy donor's plasma did not
114 show a reaction to any of these three coronaviruses (Fig. 2a). With these findings, we concluded that all
115 samples could be used for RBD-specific Abs isolation to screen NAb candidates.
116 The RBD is the key domain of SARS-CoV-2 S protein for the interaction with the human cell
117 surface receptor ACE2[9,26]. Therefore, the recombinant RBD was employed to detect the specific mB
118 cells via flow cytometry. We analyzed RBD-specific mB cells by a gating strategy of the Dead
119 $Dye^{-}CD19^{+}IgG^{+}IgD^{-}RBD^{+}$cells (Fig. 2b), the proportion of which was less than 1% in $IgD^{-}IgG^{+}$ mB
120 cells (ranging from 0.1% to 0.33%, Fig. 2c). These RBD-specific mB cells were then sorted into
121 96-well plates with one cell in each well for Ab gene isolation. Immunoglobulin heavy and light chains
122 were amplified by nested PCR from the sorted single mB cell (Fig. 3a, b). The amplified products were
123 cloned into linear expression cassettes to produce the full-length IgG1 antibodies (Fig. 3c). After three
124 rounds of screening, we obtained a total of 497 paired Ab genes from the sorted RBD-specific mB cells
125 (Supplementary Table 4).

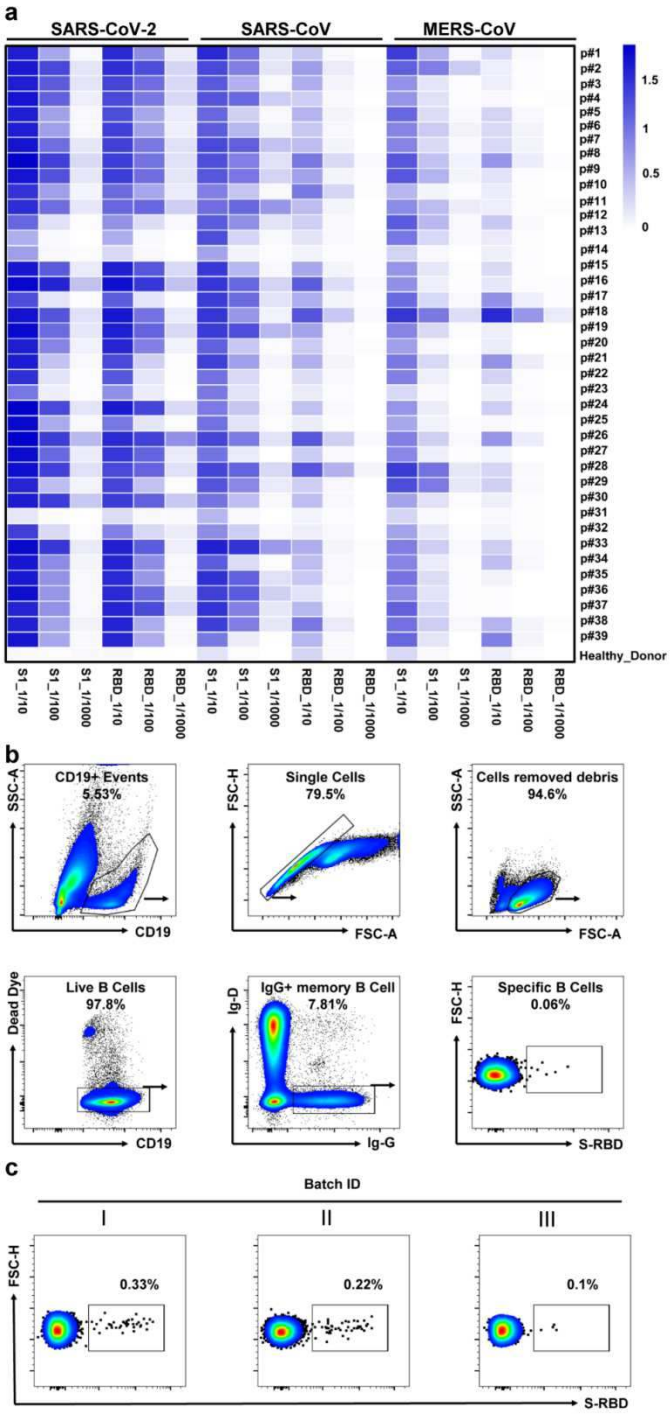

Fig. 2 Analyses of plasma response to SARS-CoV-2 and the RBD-specific memory B cells. **a** The heatmap depicts the specificity of convalescent patients' plasma against S1 or RBD of SARS-CoV-2, SARS-CoV, and MERS-CoV, with serial dilutions, measured by ELISA. The plasma of healthy donors was used as a negative control. Data were shown with the mean of representative experiments. **b** Gating strategy for SARS-CoV-2 RBD-specific IgG^+ mB cells in the PBMC of COVID-19 convalescent patients. Living $CD19^+IgD^-IgG^+$ cells were gated, and B cells binding SARS-CoV-2 RBD were selected for single-cell sorting. **c** FACS analysis of RBD-specific memory B cells in $CD19^+IgD^-IgG^+$ mB cells from the PBMC of three batches of convalescent patient samples. Plots show $CD19^+IgD^-IgG^+$ populations using the gating strategy described in **b**.

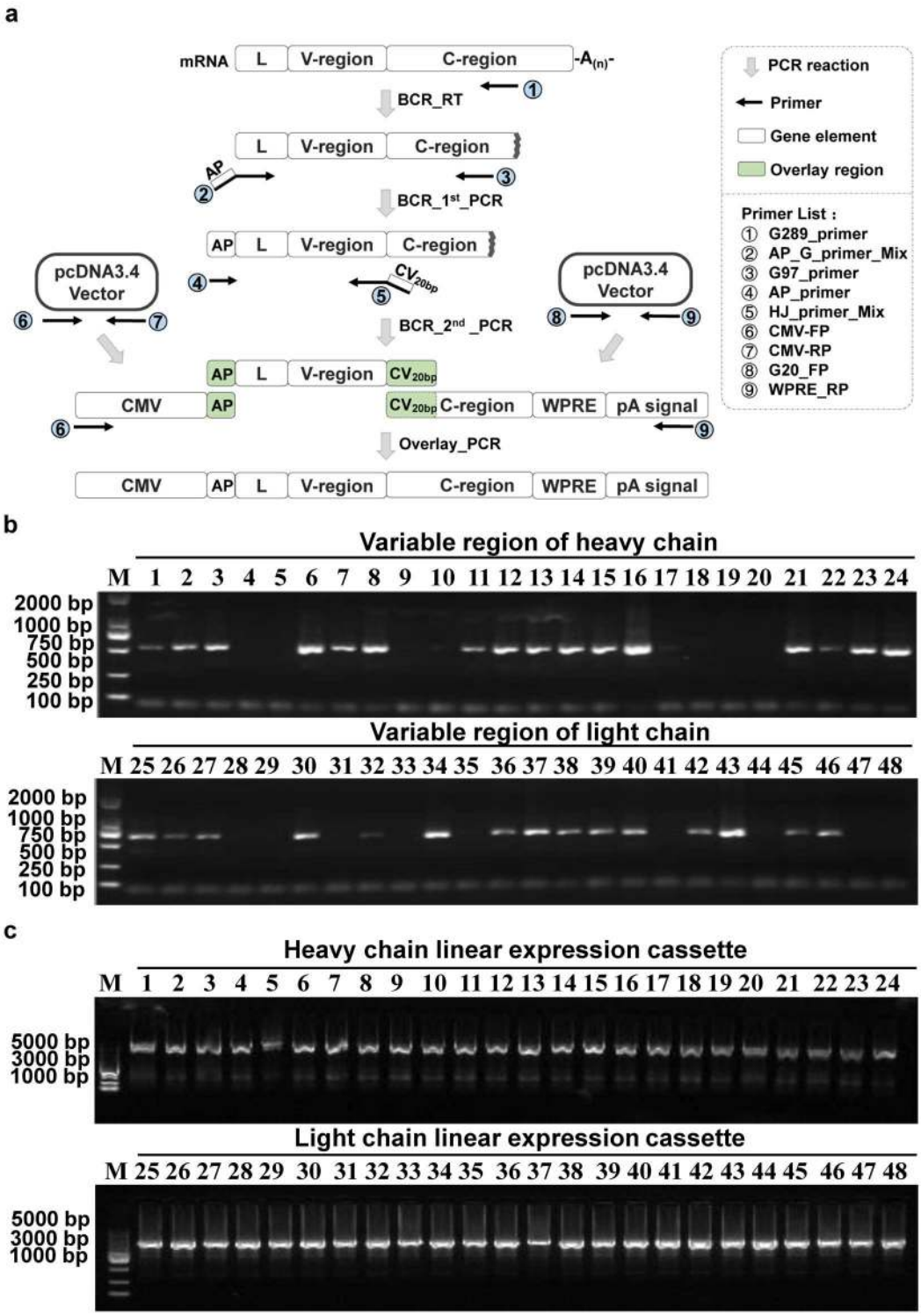

Fig. 3 Schematic diagram of the single-cell BCR Cloning and the construction of linear expression cassettes. **a** The workflow of single-cell BCR Cloning and construction of linear expression cassettes. The BCR cDNAs were obtained from the single RBD-specific mB cells by RT-PCR. the variable region of the Ab gene was amplified via the 1st and 2nd PCR, and the linear expression cassettes were constructed via the 3rd overlay PCR. 1st PCR utilized gene-specific primers at both the 5′ and 3′ ends. The 5′ forward primer including an "adapter" bound to the leader sequence of Ab cDNA (L). The 3′ reverse primer bound to the heavy or light constant regions. In the 2nd PCR, the 5′ forward primer annealed to an "adapter" locating at the 5′ end of the 1st PCR product, and the 3′ reverse primer annealed to the J gene of the Ab variable region. The 2nd PCR product provided 20

base-pair overlap regions at both sites: its 5′ end overlapping with the 3′ terminal of the human cytomegalovirus (CMV) promoter fragment and its 3′ end overlapping with the 5′ terminal of the heavy or light chain constant region fragment, which contained a polyadenylic acid sequence. Then, in the 3rd Overlay PCR, the CMV promoter fragment, the variable region fragment, and the constant region fragment were fused and amplified to produce the linear expression cassettes. **b** Agarose gel of BCR Cloning 2nd PCR product. The PCR products were electrophoresed and stained with ethidium bromide. Lane "M", 2 kb DNA ladder; Lane 1-24, the product of heavy chain variable region and Lane 25-48, the product of light chain variable region. **c,** Agarose gel of 3rd PCR product. Lane "M", 5 kb DNA ladder; Lane 1-24, linear expression cassettes of the heavy chains and Lane 25-48, linear expression cassettes of the light chains.

Assessment of the antigen reactivity and the neutralizing activity of Abs expressed by linear expression cassettes. To identify the specificity of these Abs, IgG were expressed in HEK293T cells by transient transfection of the linear expression cassettes carrying paired Ab genes. Two days later, supernatants were screened by ELISA for their binding capabilities to the recombinant S1 or RBD protein of SARS-CoV-2. In total, we identified 198 paired RBD specific antibody genes from the 497 paired Ab genes (Fig. 4a). The SARS-CoV-2 pseudovirus neutralization assay was used to assess the neutralizing abilities of these specific antibodies. Interestingly, close to 50% of these mAbs (96/198) could block the pseudovirus infection with over 75% inhibition rate (Fig. 4b), suggesting that the RBD was an ideal region to screen NAbs against SARS-CoV-2. These results have shown that our screening system can rapidly and efficiently obtain NAbs using RBD-specific mB cells.

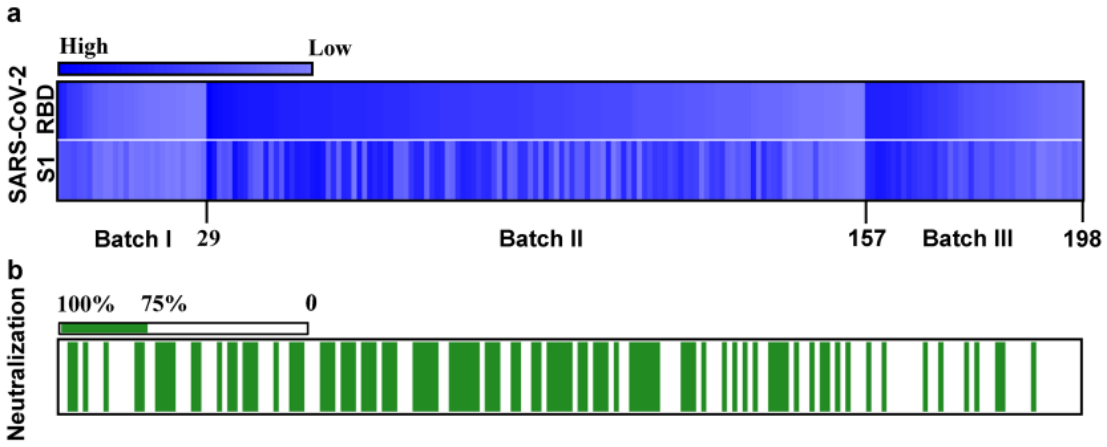

Fig. 4 Identification of RBD neutralizing antibodies from convalescent COVID-19 patients. **a** Screening of SARS-CoV-2 RBD-specific Abs. Antibodies were expressed in HEK293T cells by transfection of the linear Ab expression cassettes. Two days later, antigen reactivity of supernatants to SARS-CoV-2 S subunit S1 or RBD were tested by ELISA. The heatmap reveals that the binding ability of 198 supernatants. The brightness of blue represented the binding strength, which was reflected by the $OD_{405\ nm}$ value. The mAbs were ranked by the order of the antigen reactivity screening. **b** Screening of the potential NAbs. the neutralizing capability were identified by SARS-CoV-2 pseudovirus neutralization assay. The Green columns indicate potential neutralizing Abs (inhibition >75%), while white indicate partial or not neutralizing Abs (inhibition < 75%). The mAbs were ranked as same as the above screening order.

Characterization of RBD-specific antibody repertoire. We successfully sequenced 169 RBD-specific Abs. Among them, 158 (93.5%) were found to have unique sequences, with diverse usage of antibody variable genes (Supplementary Fig. 1, Supplementary Table 5). We analyzed the usage of antibody variable-gene segments for variable (V) genes according to the neutralizing capabilities of these 158 mAbs, tested by pseudovirus assays (Fig. 5). Abs with a neutralizing effect of over 75% against pseudovirus were termed as potential NAbs (pote-NAbs). Interestingly, we found that all mAbs with heavy chains encoded by IGHV3-66 were pote-nAbs (Fig. 5a), and IGHV3-66 gene could pair with multiple light chain V genes (IGKV1-33, IGKV1-9 and IGLV1-40) (Supplementary Fig. 1). Additionally, a large number of mAbs with light chain encoded by IGKV1-39 were pote-NAbs (Fig. 5b), and IGKV1-39 gene could pair with a bundle of heavy chains V genes to express RBD specific mAbs (Supplementary Fig. 1), which was consistent with previous reports[10,11]. We found that majority of the RBD-specific Abs were transcribed from IGHV1 to IGHV5 for the heavy chain, and IGKV1 to IGKV3 and IGLV1 to IGLV3 for the light chain (Fig. 6). Specifically, close to 50% of the pote-nAbs were transcribed from IGHV3 for the heavy chain (Fig. 6a), and IGKV1 for the light chain (Fig. 6b).

The heavy chain complementarity determining region 3 (CDRH3) is the region of an antibody with the highest diversities in amino acid sequence and length. The average length of CDRH3 in the naive human repertoire is round 15 amino acids with a normal distribution[27]. We observed that the CDRH3 lengths of the specific mAbs were mainly distributed between 11 to 19 amino acids, while the overall CDRH3 lengths matched the skew distribution (Fig. 5c). Among them, most of the potent-Abs contained 11-16 amino acids (Fig. 5c). The mean CDRH3 length in isolated SARS-CoV-2 RBD-specific mB cells differed substantially from those of other viral infections, such as HIV and influenza virus[28,29]. In terms of the CDR3 light chain (CDRL3) lengths, a range of 6 to 13 amino acids were observed, with a similar skew distribution (Fig. 5d).

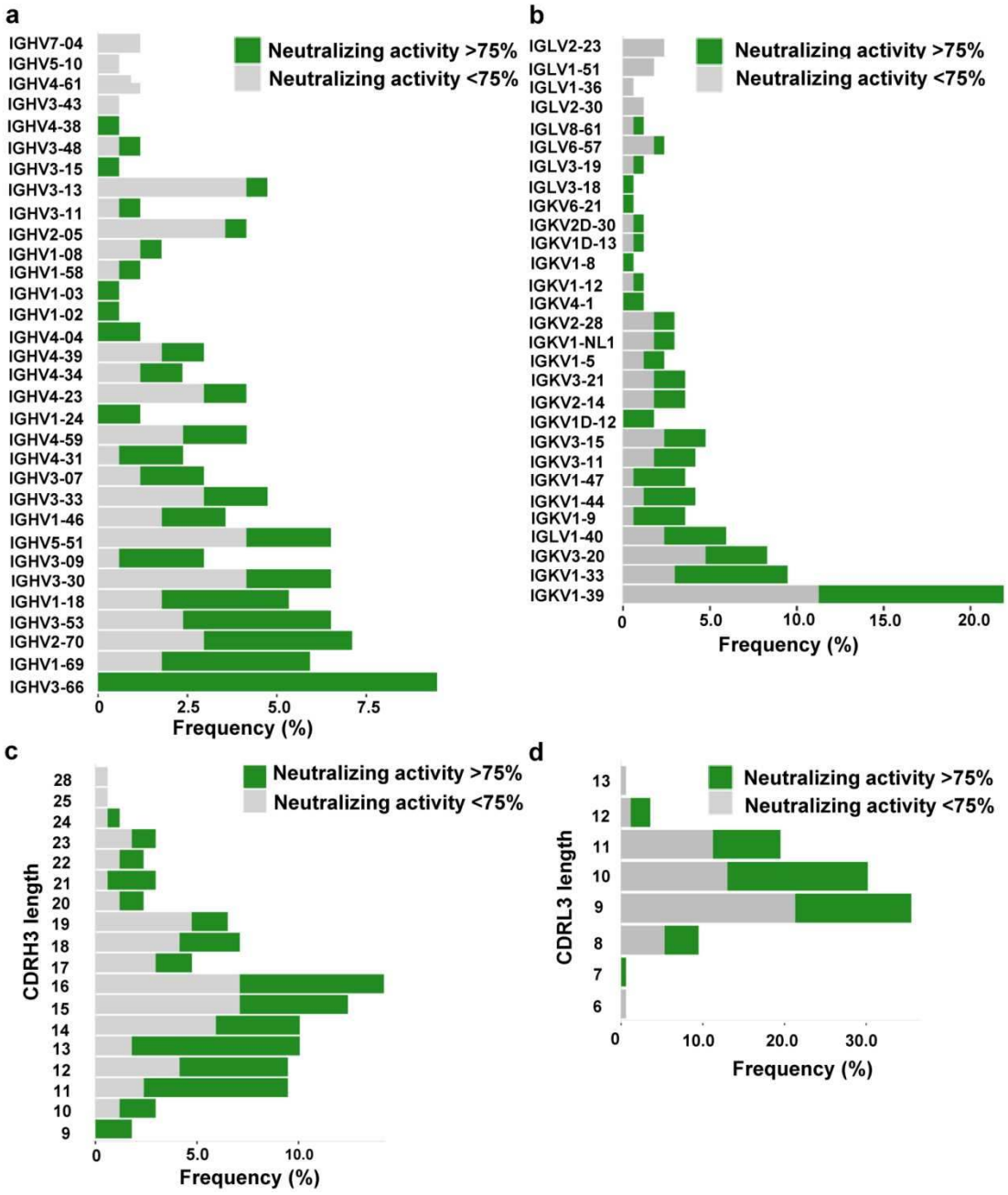

Fig. 5 Usage frequencies of the variable region gene clusters and the CDR3 lengths. **a** Usage frequencies of the variable region gene clusters of the heavy chain (VH) for the pote-NAbs and non-neutralizing Abs. 158 unique Abs sequences were used for calculating of gene frequency. **b** Usage frequencies of the variable region gene clusters of the light chain (VL) for the pote-NAbs and non-neutralizing Abs. **c** Frequencies of the heavy chain complementarity determining region 3 (CDRH3) lengths of the pote-NAbs and non-neutralizing Abs. **d** Frequencies of the light chain complementarity determining region 3 (CDRL3) lengths of the pote-NAbs and non-neutralizing Abs.

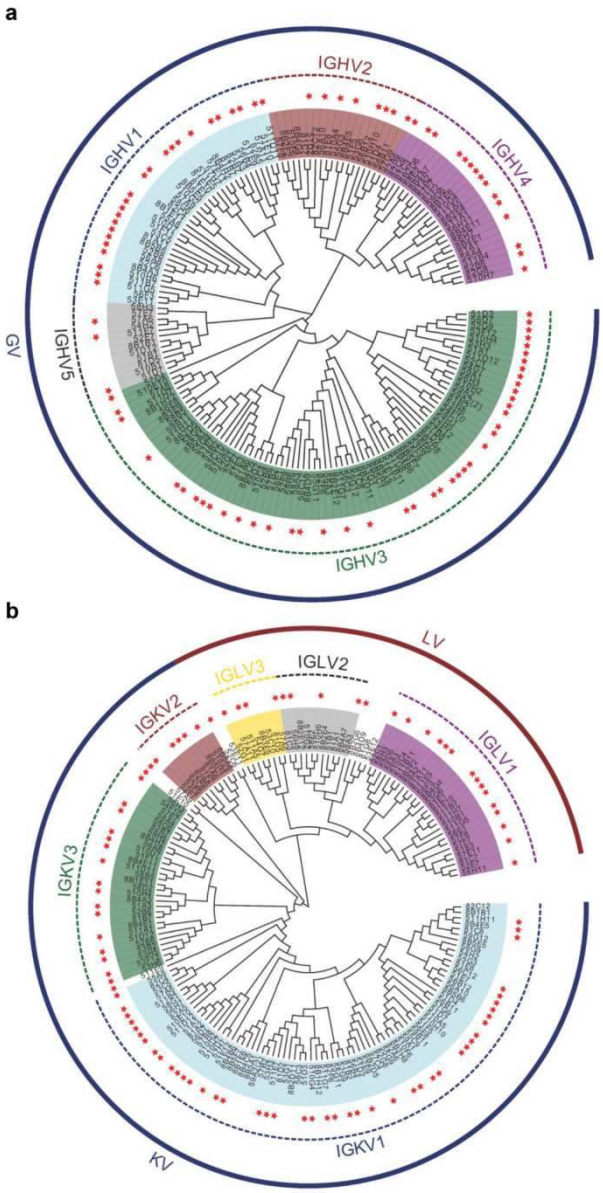

Fig. 6 Phylogenetic analysis of variable region genes in the heavy chain (VH) and the light chain (VL) for the RBD-specific mAbs. The red stars represented individual NAbs.

Identification of the potent neutralizing antibodies with high affinity. 96 pote-NAbs genes were cloned into an expression vector and transiently expressed in Expi293F cells. From a total of 96 culture supernatants, we successfully harvested 73 purified mAbs. The purified mAbs were tested for the RBD reactivity by ELISA, and we found that 65 mAbs could binding to SARS-CoV-2 S1 and SARS-CoV-2 RBD (Fig. 7a). Next, the purified mAbs were assessed their neutralizing ability *in vitro* via competitive ELISA analysis, and we found that over 70% of them could mediate blockage of ACE-2 and RBD interaction. (Fig. 7b).

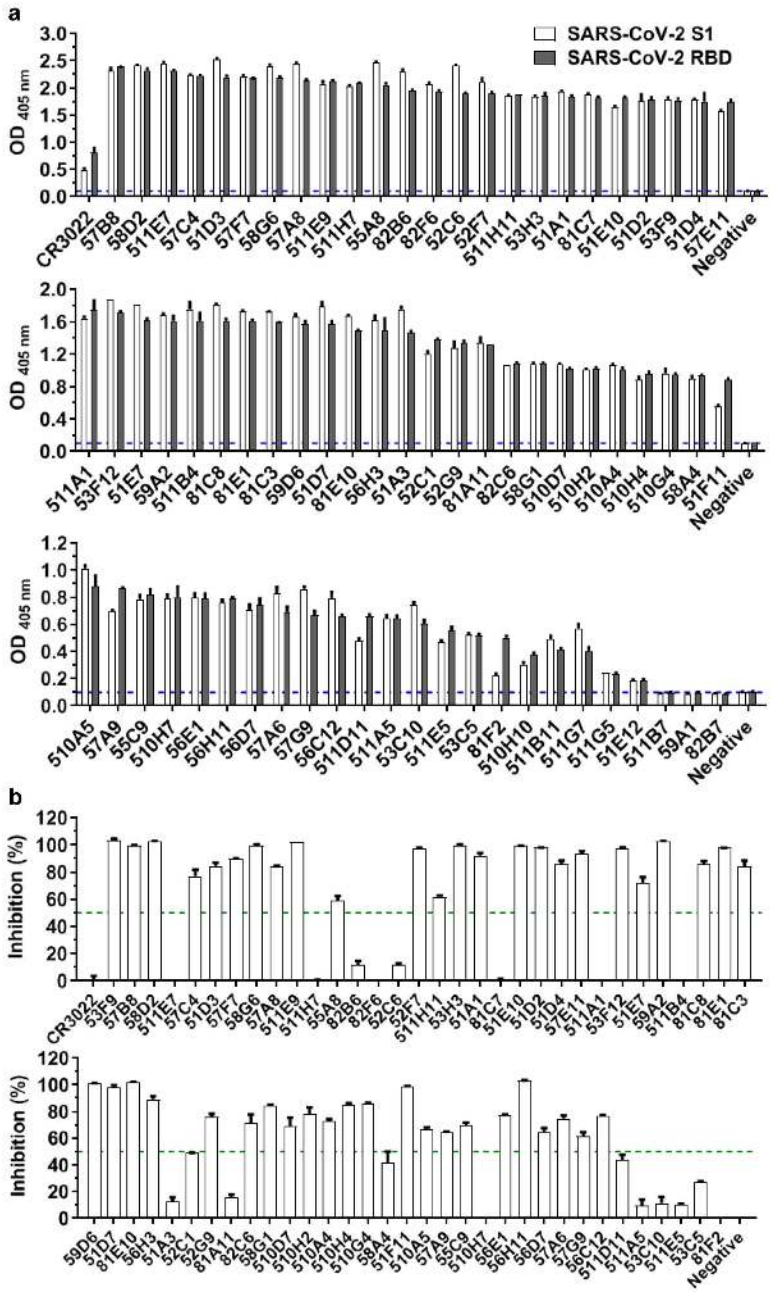

Fig. 7 The binding and blockage activity characterizations of mAbs. **a** The binding strength of purified mAbs. ELISA was used for testing binding strength, and 1 μg/ml SARS-CoV-2 S1 or RBD was coated on the 384 wells plate. The $OD_{405\ nm}$ values was measured. A SARS-CoV specific mAb (CR3022) was used as the positive control. The blue dashed lines indicated the OD_{405nm} value of negative interactions. **b** The inhibitory effect of purified mAbs against the interaction between SARS-CoV-2 RBD and ACE2, tested via competitive ELISA analysis. The green dashed lines indicated a 50% inhibition on blocking the ACE2-RBD interaction. Data were shown as mean ± SD of representative experiments.

Forty-eight purified mAbs were evaluated for their neutralizing capabilities using the authentic SARS-CoV-2 cytopathic effect (CPE) inhibition assay, and the results were listed according to the order of inhibitory ability (Fig. 8a). Among them, 20 mAbs were able to completely block the authentic SARS-CoV-2 infection with a concentration of 1 μg/ml, and the top 2 mAbs (58G6, 510A5) could

completely inhibit the authentic SARS-CoV-2 infection below 0.14 μg/ml. Furthermore, half-maximal inhibitory concentration (IC_{50}) values of 58G6 and 510A5 were determined by RT-qPCR method using authentic SARS-CoV-2 virus infection. We found that the IC_{50} values of 58G6 and 510A5 were 9.98 and 11.13 ng/ml, respectively (Fig. 8b). Moreover, we tested the binding affinity of 58G6 and 510A5 to SARS-CoV-2 RBD via the surface plasmon resonance (SPR) assay. Equilibrium constant (Kd) of 58G6 and 510A5 were 0.385 nM and 7.8 nM (Fig. 8c). Therefore, using our screening system, the most potent neutralizing mAbs (58G6 and 510A5) were obtained and could be used as candidate biologics to prevent or treat SARS-CoV-2 infection.

a

Number	mAb	Concentration (μg/ml) 18.76	9.38	4.69	2.35	1.17	0.59	0.29	0.14
1	58G6	-	-	-	-	-	-	-	-
2	510A5	-	-	-	-	-	-	-	-
3	13G9*	-	-	-	-	-	-	-	-
4	510A4	-	-	-	-	-	-	-	++
5	51D3	-	-	-	-	-	-	+	++
6	55A8	-	-	-	-	-	-	+	++
7	51A1	-	-	-	-	-	-	+	+++
8	81E1	-	-	-	-	-	-	+	+++
9	51E10	-	-	-	-	-	-	+	+++
10	51D7	-	-	-	-	-	-	+	+++
11	07C1	-	-	-	-	-	+	+	+++
12	53H3	-	-	-	-	-	+	+	+++
13	52F7	-	-	-	-	-	+	+	+++
14	57B8	-	-	-	-	-	+	++	+++
15	57F7	-	-	-	-	-	+	++	+++
16	51D4	-	-	-	-	-	+	++	+++
17	55C9	-	-	-	-	-	+	++	+++
18	56D7	-	-	-	-	-	+	++	+++
19	510H2	-	-	-	-	-	+	++	+++
20	81C3	-	-	-	-	-	+	++	+++
21	53F12	-	-	-	-	+	+	+++	+++
22	82A6	-	-	-	-	+	+	++	++++
23	51D2	-	-	-	-	+	++	+++	++++
24	57E11	-	-	-	-	+	++	+++	++++

Number	mAb	Concentration (μg/ml) 18.76	9.38	4.69	2.35	1.17	0.59	0.29	0.14
25	57A9	-	-	-	-	+	++	+++	++++
26	58G1	-	-	-	-	+	++	+++	++++
27	510D7	-	-	-	-	+	++	+++	++++
28	510H4	-	-	-	-	+	++	+++	++++
29	52C6	-	-	-	+	+	+++	++++	++++
30	510H7	-	-	-	+	++	+++	++++	++++
31	56E1	-	-	-	+	++	+++	++++	++++
32	56H3	-	-	-	+	++	+++	++++	++++
33	51F11	-	-	-	+	++	+++	++++	++++
34	57C4	-	-	+	++	+++	++++	++++	++++
35	07B7	-	-	+	++	+++	++++	++++	++++
36	82F6	-	+	++	+++	++++	++++	++++	++++
37	511G7	-	+	++	+++	++++	++++	++++	++++
38	51E7	-	+	++	+++	++++	++++	++++	++++
39	57A6	-	+	++	+++	++++	++++	++++	++++
40	52G9	+	+	++	+++	++++	++++	++++	++++
41	56C12	+	++	+++	++++	++++	++++	++++	++++
42	510G4	+	+++	++++	++++	++++	++++	++++	++++
43	81C8	+	+++	++++	++++	++++	++++	++++	++++
44	511A5	+	+++	++++	++++	++++	++++	++++	++++
45	511B4	+	+++	++++	++++	++++	++++	++++	++++
46	57A8	++	+++	++++	++++	++++	++++	++++	++++
47	57G9	++	++++	++++	++++	++++	++++	++++	++++
48	51E12	++++	++++	++++	++++	++++	++++	++++	++++

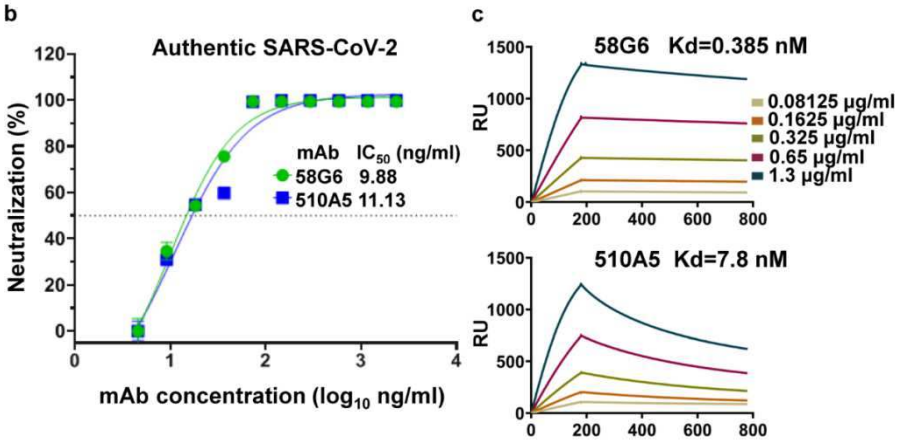

Fig. 8 Functional characterization of NAbs against authentic SARS-CoV-2. **a** The neutralization activities of mAbs against authentic SARS-CoV-2 virus (nCoV-SH01), analyzed by the Cytopathic effects (CPE) test. Serial dilutions of each mAbs were tested, ranging from 18.76 μg/ml to 0.14 μg/ml. CPE results was summarized in (A), where "++++" indicates 100% cytopathy, "+++" indicates 50-75% cytopathy, "++" indicates 25-50% cytopathy, "+" indicates <25% cytopathy and "-" indicates no cytopathy. 13G9 was marked with "*" to indicate that it was obtained by the method previously described[30]. **b** IC_{50} of 58G6 and 510A5 against the authentic SARS-CoV-2 virus, determined in Vero-E6 cells by RT-qPCR. Dashed lines indicated a 50% inhibition rate of viral infection. Data were shown as mean ± SD of representative experiments. **c** Binding kinetics of 58G6 (top)

and 510A5 (bottom) to SARS-CoV-2 RBD, measured by Surface Plasmon Resonance (SPR). The purified mAbs was captured onto the CM5 sensor chip coating with anti-human IgG-Fc Ab, followed by the injection of soluble SARS-CoV-2 RBD at five different concentrations. The x-axis represents seconds. The results are representatives of two independent experiments.

Discussion

Neutralizing antibody-based therapeutic is an ideal medicine for treatment and prevention of the infectious diseases[31]. Although NAbs against SASR-CoV-2 could be obtained from convalescent patients, the success rate to discover potent NAbs with therapeutic promise remains undesired. In this study, we described a strategically optimized screening method to discover potent mAbs from a large number of the antigen specific Abs.

Compared with conventional methods for screening NAbs[11,20-22], several strategic optimizations of our screening system were discussed below (Supplementary Fig. 2). Firstly, we utilized the RBD of SARS-CoV-2 as bait to label specific mB cells, which would usually experience affinity maturation and somatic hypermutation[32,33]. SARS-CoV-2 RBD has been proven to be essential for the ACE2-binding during virus entry[8]. Although SARS-CoV-2 S could also be applied as bait, it could bring a large number of non-neutralizing antibodies derived from non-RBD regions[13,18,19]. Secondly, we pooled PBMCs from 5-7 convalescent patients for sorting RBD-specific mB cells. This could reduce duplicated clones to only 6.5% in total, as compared to approximately 20% in other studies[13,21], and improve the overall screening efficiency. Thirdly, we found that removing dead cells was an essential step for sorting extremely rare RBD specific mB cells, which was less than 1% of the $CD19^{+}IgD^{-}IgG^{+}$ mB cells, and this could improve the efficiency of the single-B cell receptor (BCR) amplification (Supplementary Fig. 3).

Moreover, we optimized multiple steps for the single cell BCR cloning and expression[34,35] (Fig. 3a, Supplementary Table 1,2). In the first step, we designed primers targeting the initial 20 nucleotides at the 5' end of the signal peptide of Ab genes as the forward primers, which can reduce the loss of BCR clones caused by SNP at the primer binding sites. Next, PCR products containing the adaptor primers could be used for the simultaneous construction of linear gene expression cassettes and plasmids without the extra-modification. Also, with Ab J-region primers in the 2^{nd} PCR, we were able to improve the recombination efficiency of linear cassettes to approaching 100%. Construction of the linear expression cassettes instead of plasmids could drastically reduce the workload and time. Lastly, preliminary evaluation of neutralization activity on, as early as, the sixth day could filter and re-size

our Ab pools to be applied in the subsequent steps, making a great improvement with overall efficiency.

Using this optimized screening system, we efficiently generate a panel of NAbs with relatively great potency. When we analyzed the distribution of gene clusters of BCR repertoire of potential neutralizing and non-neutralizing antibody sequences, a few interesting observations were found. Our results revealed that potential NAbs tended to be distributed in several gene clusters, such as VH3-66 and VH3-53, etc., among which, the VH3-66 cluster exclusively produced NAbs. This result may be helpful in analyzing the preference distribution of genes encoding NAbs in the future. Meanwhile, CDRH3 length is reported as a key factor to value the diversity of RBD specific Abs, due to the changeable amino acid compositions. We found that the CDRH3 lengths of potential NAbs showed a skewed distribution, with an inclined length of 11-16 amino acids. It suggested that the SARS-CoV-2 Abs were likely derived from mB cells during the primary response to SARS-CoV-2 infection but not a recall response to SARS-CoV or MERS-CoV, even though our collected blood specimens were cross-reactive with both SARS-CoV and MERS-CoV S proteins[28].

One additional improvement that may be integrated into our screening system is the single-cell sequencing method. The development of proper algorithms to evaluate neutralization capabilities with the incorporation of heavy chain variable region preferences, for example, IGHV3-66, could help to precisely predict NAbs from repertoires containing thousands of antigen specific mAb[14,15]. This might further provide desired candidates of NAbs with potential therapeutic value, with better time-efficiency and economical preferences.

Based on the screening strategy described above, we successfully identified 20 potent NAbs that can completely block authentic SARS-CoV-2 virus infection at 1.17 μg/ml. The top two antibodies (58G6 and 510A5) both generated IC_{50} at around 10 ng/ml, with high binding affinity to SARS-CoV-2 RBD, which were found to be some of the most potent NAbs discovered to date. In conclusion, we have successfully established an optimized screening system for NAbs, which can generate a large number of desired NAbs against SARS-CoV-2 in a total period of 15 days. Our screening system could be expanded to other infectious diseases and serve as a fundamental methodology for discovering NAbs for emerging infectious diseases.

Materials and Methods

Isolation of single RBD-specific memory B cells by FACS. PBMCs from the convalescent patients were thawed and rested overnight. The mixed samples staining as following. 2 μg/ml RBD-his in 200 μl PBS (added with 2% FBS) was mixed with the specific antibody cocktail required for staining B cell. Then these PBMCs was incubated with a mixed antibodies cocktail at 4 °C for 30 min (the antibodies cocktail including FITC-anti-human CD19 antibody (Biolegend, clone: SJ25C1), BV421-anti-human IgD antibody (Biolegend, clone: IA6-2), PerCP-Cy5.5-anti-human IgG antibody (Biolegend, clone: M1310G05), APC-anti-his tag antibody (Biolegend, clone: J095G46)). Dead dye (LIVE/DEAD™ Fixable Near-IR Dead Cell Stain Kit, Thermo Fisher) was added at 4 °C for 20 min. After washing the cells, the FACS analysis was performed by BD FACSAria III Cell Sorter (BD Biosciences) with FSC-A versus SSC-A identifying cell population, FSC-A versus FSC-H excluding doublets. Then FSC-H versus Dead Dye was gated to remove dead cells. RBD-specific single memory B cells were gated by $CD19^{+}IgD^{-}IgG^{+}His^{+}$, and single-cell sorted into 96-well PCR plates (free of DNase and RNase, Bio-Rad). The Plates were stored at -80 °C until BCR Cloning. Data analysis was performed utilizing the FlowJo software (FlowJo, LLC).

Amplification of single-cell BCR variable region. Our primers for PCR were designed from leader sequences and J region sequence of immunoglobulin (Ig) annotated by the IMGT reference directory (http://www.imgt.org/vquest/refseqh.html). An adaptor sequence was added to the 5′ end of the leader primers for the 2nd PCR. 31 leader primers (AP_G_leader Mix) was designed for the heavy chain of Ig, and 19 leader primers (AP_K_leader Mix) was used in the amplification of the kappa chain of Ig, and 21 leader primers (AP_L_leader Mix) for the lambda chain of Ig were designed. For the initial step of RT-PCR, 5 μl of the RT_Mix_A was added into each well of 96 well plates containing a single B cell. Then the mixture was incubated at 65℃ for 5 min and put on ice immediately for 3 min. 5 μl RT_Mix_B was added into each well of the plate with reaction program: 45 ℃ for 45 min, 70 ℃ for 15 min. 1 μl of RT product was moved to the well of a new 96 well plate containing 9 μl 1st PCR Mix Gamma /Kappa/Lamda, respectively. The PCR program for 1st PCR: 95℃ for 3 min, 30 cycles of 95℃ for 10 sec, 55℃ for 5 sec, and 72℃ for 1 min. 1 μl of the tenfold-diluted 1st PCR product was then added into each well of a new 96 well plate holding 9 μl 2nd PCR Mix Gamma/Kappa/Lamda, respectively. The PCR program for 2nd PCR: 95℃ for 3 min, 35 cycles of 95℃ for 10 sec, 55℃ for 5 sec, and 72℃ for 45 sec. The second PCR products were further cloned into the antibody linear

expression cassettes or expression vectors to express full IgG1 antibodies. PCR reaction Mixtures are prepared as described in Supplementary Table 6. All of the PCR primers are listed in Supplementary Table 1 and prepared in Supplementary Table 7.

Generation of linear antibody expression cassettes and expression of Abs. 2nd PCR products were used to ligate with the expression cassettes directly by overlapping PCR. The products were purified with the ethanol precipitation method. Briefly, 120 μl of absolute ethanol and 6 μl of 3 M sodium acetate were mixed with 60 μl of the Overlap PCR product. Then the reagents were incubated at -80 °C for 30 minutes. After centrifuging at 10,000 rpm for 20 minutes, the supernatant was discarded the and the pellet adhered on the tube were rinsed with 200 μl 70% ethanol and absolute ethanol and evaporated the ethanol at 56°C for 10 min. 40 μl sterile water was added to dissolve the DNA pellet. After measuring the nucleic acid concentration, purified overlapping PCR products of paired heavy and light chain expression cassettes were co-transfected in HEK293T cells. The binding ability of transfected culture supernatants to SARS-CoV-2 RBD was tested by ELISA after 48 hours.

Recombinant antibody production and purification. For the construction of antibody expression Vectors, VH and VL 2nd PCR products were inserted separately into the linearized plasmids (pcDNA3.4) that encode constant regions of the heavy chains and light chains via a homologous recombination kit (Catalog No. C112, Vazyme). A pair of plasmids separately expressing heavy and light chain of antibodies were transiently co-transfected into Expi293™ cells (Catalog No. A14528, ThermoFisher) with ExpiFectamine™ 293 Reagent. Then the cells were cultured in a shaker incubator at 120 rpm and 8% CO_2 at 37 ℃. After 7 days, the supernatants with the secretion of antibodies were collected and captured by protein G Sepharose (GE Healthcare). The bound antibodies on the Sepharose were eluted and dialyzed into phosphate-buffered saline (PBS). The purified antibodies were used in following binding and neutralization analyses.

ELISA binding assay and competitive ELISA. 2 μg/ml the recombinant S or RBD proteins derived from SARS-CoV-2, SARS-CoV, or MERS-CoV (Sino Biological, Beijing) were coated on 384-well plates (Corning) at 4°C overnight. Plates were blocked with blocking buffer (PBS containing 5% FBS and 2% BSA) at 37°C for 1 hour. Serially diluted convalescents' plasma or mAbs were added into the plates and incubated at 37°C for 30 min. Plates were washed with phosphate-buffered saline, 0.05% Tween-20 (PBST) and ALP-conjugated goat anti-human IgG (H+L) antibody (Thermo Fisher) was added into each well and incubated at 37°C for 1 hour. Lastly, the PNPP substrate was added, and

absorbance was measured at 405 nm by a microplate reader (Thermo Fisher). For a competitive ELISA to test the effect of mAbs on blocking ACE2 binding RBD, 2 μg/ml the recombinant ACE2 (Sino Biological, Beijing) was added in 384-well plates and overnight at 4°C, followed by blocking with the blocking buffer and washing. 500 ng/ml RBD-mouse-Ig-Fc was pre-incubated with test specimen at 37°C for 1 hour, followed by adding into the wells coated with ACE2 and incubated at 37°C for 1 hour. Unbound antigen was removed with washes. Then ALP-conjugated anti-mouse-Ig-Fc antibody was added into the wells and incubated at 37°C for 30 min. PNPP was added and measured as above.

Pseudovirus neutralization assay. Pseudovirus was generated as previously described[36]. HEK293T cells were transfected with psPAX2, pWPXL Luciferase, and pMD2.G plasmid encoding either SARS-CoV-2 S. The supernatants were harvested 48 hours later, filtered by 0.45 μm filter and centrifugated at 300 g for 10 min to collect the supernatant and then aliquoted and storied at -80°C. The purified antibodies with serial dilution were incubated with pseudovirus at 37°C for 1 hour. The mixture of viruses and specimens was then added in a hACE2 expressing cell line (hACE2-293T cell). After 48 hours culture, the luciferase activity of infected hACE2/293T cells was measured by the Bright-Luciferase Reporter Assay System (Promega). Relative luminescence units (RLU) of Luc activity was detected using the ThermoFisher LUX reader. All experiments were performed at least three times and expressed as means ± standard deviations (SDs). Half-maximal inhibitory concentrations (IC_{50}) were calculated using the four-parameter logistic regression in GraphPad Prism 8.0.

Authentic SARS-CoV-2 virus neutralization assays. An authentic SARS-CoV-2 neutralization assay was performed in a biosafety level 3 laboratory of Fudan University. Serially diluted mAbs were incubated with authentic SARS-CoV-2 (nCoV-SH01, GenBank: MT121215.1, 100 TCID50) at 37°C for 1 hour. After incubation, the mixtures were then transferred into 96-well plates, which were seeded with Vero E6 cells. After incubation at 37°C for 48 hours, each well was examined for CPE and supernatant viral RNA by RT-qPCR. For RT-qPCR, the viral RNA was extracted from the collected supernatant using Trizol LS (Invitrogen) and used as templates for RT-qPCR analysis by Verso 1-step RT-qPCR Kit (Thermo Scientific) following the manufacturer's instructions. PCR primers targeting SARS-CoV-2 N gene (nt608-706) were as followed (forward/reverse): 5′-GGGGAACTTCTC CTGCTAGAAT-3′/5′-CAGACATTTTGCTCTCAAGCTG-3′. qRT-PCR was performed using the

LightCycler 480 II PCR System (Roche) with the program as followed: 50°C 15 min; 95°C 15 min; 40 cycles of 95°C 15 sec, 50°C 30 sec, 72°C 30 sec.

Antibody binding affinity measurement by SPR. The affinity of antibody binding SARS-Cov-2-S-RBD was measured via the Biacore X100 platform. The CM5 chip (GE Healthcare) was coupled with an anti-human IgG-Fc antibody to capture 9000 RU antibodies. Gradient concentrations of SARS-Cov-2 RBD (Sino Biological Inc.) were diluted (2-fold dilution, from 50 nM to 0.78 nM) with HBS-EP$^+$ Buffer (0.01 M HEPES, 0.15 M NaCl, 0.003 M EDTA and 0.05% (v/v) Surfactant P20, pH 7.4), then injected into the human IgG capturing chip. The sensor surface was regenerated with 3 M magnesium chloride at the end of each cycle. The affinity was calculated using a 1:1 binding fit model in Biacore X100 Evaluation software (Version:2.0.2).

Sequence analysis of antigen-specific mAb sequences. IMGT/V-QUEST (http://www.imgt.org/IMGT_vquest /v quest) and Ig BLAST (https://www.ncbi.nlm.nih.gov/igblast/), MIXCR (https://mixcr.readthedocs.io/en/master/) and VDJ tools (https://vdjtools-doc.readthedocs.io/en/master/overlap.html) tools were used to do the VDJ analysis and annotation, germline divergence for each antibody clone. The Phylogeny tree analysis of IgG heavy and light chain variable genes was performed with Mega X (Molecular Evolutionary Genetics Analysis across computing platforms) by the Maximum Likelihood method. Abs DNA sequences were compared with each other by Clustal W (pairwise alignments) to analyze sequence similarity, and EvolView (https://www.evolgenius.info/evolview/) was used for the decoration of Phylogeny tree. R packages (ggplot2, p heatmap) were used for the bar chart, heatmap and Cicos plot.

Ethics Statement. The project “The application of antibody tests patients infected with SARS-CoV-2” was approved by the ethics committee of Chongqing Medical University. Informed consents were obtained from all participants.

Acknowledgments: We acknowledge the work and contribution of blood sample providers from Chongqing Medical University affiliated Yongchuan Hospital and the third affiliated Hospital of Chongqing Medical University. We also thank health donors from Chongqing Medical University. This study was supported by Chongqing Medical University fund (X4457) with the donation from Mr. Yuling Feng.

Author contributions

A.J. and A.H. conceived and designed the study, K.D. and F.G. offered help on the collection of convalescent patient blood samples. X.H. performed the fluorescence-activated cell sorting. X.H., C.H., L.L. and Q.C. performed the single B cell PCR experiments. Y.W., R.W, F.G., J.H., S.M., Y.L., S.S. and Y.H. constructed the linear antibodies gene expression cassettes. F.L. and H.J. were responsible for antibody expression and purification. J.W., K.W., J.H., S.L., N.T., G.Z. and Q.G. conducted the pseudovirus neutralization assays, Y.X., C.G., Y.W., W.X., X.C., D.Q. and Z.Y. performed authentic SARS-CoV-2 neutralization assays. S.L., M.S., Y.W., X.H. and A.J. analyzed the antibody sequences. S.L., M.S., Y.W., W.W, X.H. and J.W. generated figures and tables, and take responsibility for the integrity and accuracy of data presentation. X.H., A.J., and W.W. wrote the manuscript.

Data availability statements All information presented in this study will be upload soon.

Conflict of interests: Patent has been filed for some of the antibodies presented here.

References

1. Chen, N.*, et al.* Epidemiological and clinical characteristics of 99 cases of 2019 novel coronavirus pneumonia in Wuhan, China: a descriptive study. *The Lancet* **395**, 507-513 (2020).
2. Cummings, M.J.*, et al.* Epidemiology, clinical course, and outcomes of critically ill adults with COVID-19 in New York City: a prospective cohort study. *The Lancet* **395**, 1763-1770 (2020).
3. Wang, C., Horby, P.W., Hayden, F.G. & Gao, G.F. A novel coronavirus outbreak of global health concern. *The Lancet* **395**, 470-473 (2020).
4. de Wit, E., van Doremalen, N., Falzarano, D. & Munster, V.J. SARS and MERS: recent insights into emerging coronaviruses. *Nature Reviews Microbiology* **14**, 523-534 (2016).
5. Mair-Jenkins, J.*, et al.* The effectiveness of convalescent plasma and hyperimmune immunoglobulin for the treatment of severe acute respiratory infections of viral etiology: a systematic review and exploratory meta-analysis. *The Journal of infectious diseases* **211**, 80-90 (2015).
6. Ko, J.H.*, et al.* Challenges of convalescent plasma infusion therapy in Middle East respiratory coronavirus infection: a single centre experience. *Antiviral therapy* **23**, 617-622 (2018).
7. Iwasaki, A. & Yang, Y. The potential danger of suboptimal antibody responses in COVID-19. *Nature Reviews Immunology* **20**, 339-341 (2020).
8. Walls, A.C.*, et al.* Structure, Function, and Antigenicity of the SARS-CoV-2 Spike Glycoprotein. *Cell* **181**, 281-292.e286 (2020).
9. Hoffmann, M.*, et al.* SARS-CoV-2 Cell Entry Depends on ACE2 and TMPRSS2 and Is Blocked by a Clinically Proven Protease Inhibitor. *Cell* **181**, 271-280.e278 (2020).
10. Hansen, J.*, et al.* Studies in humanized mice and convalescent humans yield a SARS-CoV-2 antibody cocktail. *Science* (2020).
11. Zost, S.J.*, et al.* Rapid isolation and profiling of a diverse panel of human monoclonal antibodies targeting the SARS-CoV-2 spike protein. *Nat Med* (2020).

12. Zost, S.J., *et al.* Potently neutralizing and protective human antibodies against SARS-CoV-2. *Nature* (2020).
13. Brouwer, P.J.M., *et al.* Potent neutralizing antibodies from COVID-19 patients define multiple targets of vulnerability. *Science* **369**, 643-650 (2020).
14. Cao, Y., *et al.* Potent Neutralizing Antibodies against SARS-CoV-2 Identified by High-Throughput Single-Cell Sequencing of Convalescent Patients' B Cells. *Cell* **182**, 73-84 e16 (2020).
15. Liu, L., *et al.* Potent neutralizing antibodies against multiple epitopes on SARS-CoV-2 spike. *Nature* (2020).
16. Tian, X., *et al.* Potent binding of 2019 novel coronavirus spike protein by a SARS coronavirus-specific human monoclonal antibody. *Emerg Microbes Infect* **9**, 382-385 (2020).
17. Wu, Y., *et al.* A noncompeting pair of human neutralizing antibodies block COVID-19 virus binding to its receptor ACE2. *Science* **368**, 1274-1278 (2020).
18. Chi, X., *et al.* A neutralizing human antibody binds to the N-terminal domain of the Spike protein of SARS-CoV-2. *Science* **369**, 650-655 (2020).
19. Kreer, C., *et al.* Longitudinal Isolation of Potent Near-Germline SARS-CoV-2-Neutralizing Antibodies from COVID-19 Patients. *Cell* (2020).
20. Shi, R., *et al.* A human neutralizing antibody targets the receptor-binding site of SARS-CoV-2. *Nature* **584**, 120-124 (2020).
21. Ju, B., *et al.* Human neutralizing antibodies elicited by SARS-CoV-2 infection. *Nature* **584**, 115-119 (2020).
22. Wang, C., *et al.* A human monoclonal antibody blocking SARS-CoV-2 infection. *Nat Commun* **11**, 2251 (2020).
23. Baum, A., *et al.* Antibody cocktail to SARS-CoV-2 spike protein prevents rapid mutational escape seen with individual antibodies. *Science* (2020).
24. Liao, H.X., *et al.* High-throughput isolation of immunoglobulin genes from single human B cells and expression as monoclonal antibodies. *J Virol Methods* **158**, 171-179 (2009).
25. Long, Q.-X., *et al.* Antibody responses to SARS-CoV-2 in patients with COVID-19. *Nature Medicine* **26**, 845-848 (2020).
26. Yan, R., *et al.* Structural basis for the recognition of SARS-CoV-2 by full-length human ACE2. *Science* **367**, 1444-1448 (2020).
27. Briney, B., Inderbitzin, A., Joyce, C. & Burton, D.R. Commonality despite exceptional diversity in the baseline human antibody repertoire. *Nature* **566**, 393-397 (2019).
28. Yu, L. & Guan, Y. Immunologic Basis for Long HCDR3s in Broadly Neutralizing Antibodies Against HIV-1. *Front Immunol* **5**, 250 (2014).
29. Wu, N.C., *et al.* In vitro evolution of an influenza broadly neutralizing antibody is modulated by hemagglutinin receptor specificity. *Nature Communications* **8**, 15371 (2017).
30. Jin, A., *et al.* A rapid and efficient single-cell manipulation method for screening antigen-specific antibody-secreting cells from human peripheral blood. *Nat Med* **15**, 1088-1092 (2009).
31. Jiang, S., Hillyer, C. & Du, L. Neutralizing Antibodies against SARS-CoV-2 and Other Human Coronaviruses. *Trends in Immunology* **41**, 355-359 (2020).
32. Phan, T.G. & Tangye, S.G. Memory B cells: total recall. *Current opinion in immunology* **45**, 132-140 (2017).

33. Akkaya, M., Kwak, K. & Pierce, S.K. B cell memory: building two walls of protection against pathogens. *Nature Reviews Immunology* **20**, 229-238 (2020).
34. Tiller, T.*, et al.* Efficient generation of monoclonal antibodies from single human B cells by single cell RT-PCR and expression vector cloning. *J Immunol Methods* **329**, 112-124 (2008).
35. Smith, K.*, et al.* Rapid generation of fully human monoclonal antibodies specific to a vaccinating antigen. *Nat Protoc* **4**, 372-384 (2009).
36. Ou, X.*, et al.* Characterization of spike glycoprotein of SARS-CoV-2 on virus entry and its immune cross-reactivity with SARS-CoV. *Nature Communications* **11**, 1620 (2020).

Figures

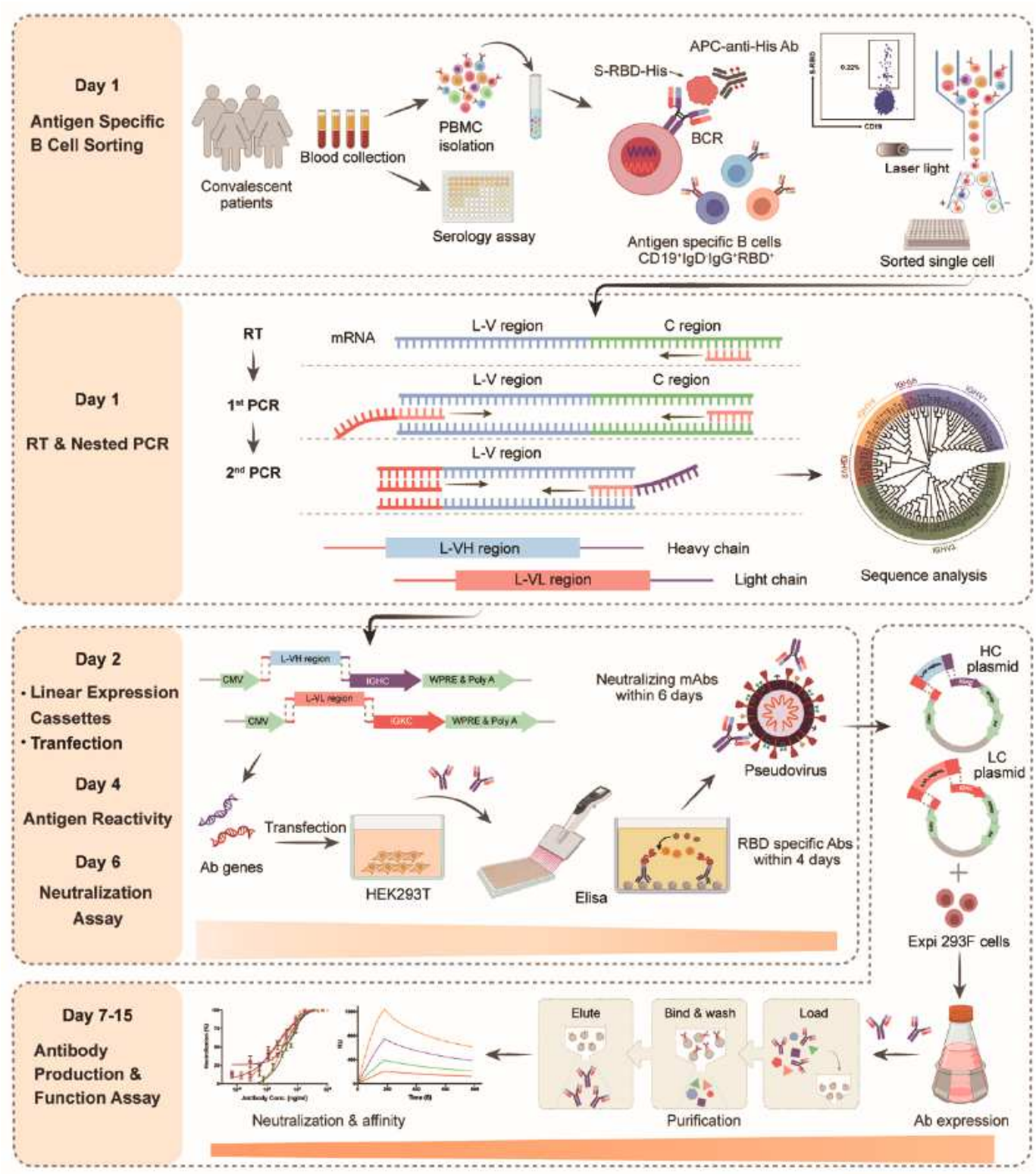

Figure 1

Schematic overview of the rapid and efficient NAbs screening system. Rapid NAbs screening workflows and timelines are shown, representing the multiple processes conducted in order. The PBMC were isolated from collected convalescent patients' blood, and the RBD-specific memory B cells in the PBMC were

sorted as single cells via flow cytometry (day 1). Then, the IgG heavy and light chains of mAb genes were amplified by RT-PCR on the same day. 2nd PCR products were cloned into the linear expression cassettes (day 2). HEK293T cells expressed antibodies by transient transfection with equal amounts of paired heavy and light chain linear expression cassettes and culture for 48 hours. The supernatants were used to detect the antigen reactivity of antibodies by ELISA in 384-well plates (day 4). The neutralizing activities of antibodies were measured with pseudovirus bearing SARS-CoV-2 S in 96-well plates (day 6). Plasmids expressing potential NAbs were transfected into Exi293F cells for the large-scale production of Ab proteins. The cell supernatants of Exi293F cells were collected, and the antibody proteins were purified by protein G beads. Antigen reactivity, neutralizing activity, and binding affinity were further accessed via ELISA, competitive ELISA, and surface plasmon resonance (SPR). Figures were created with Biorender.com.

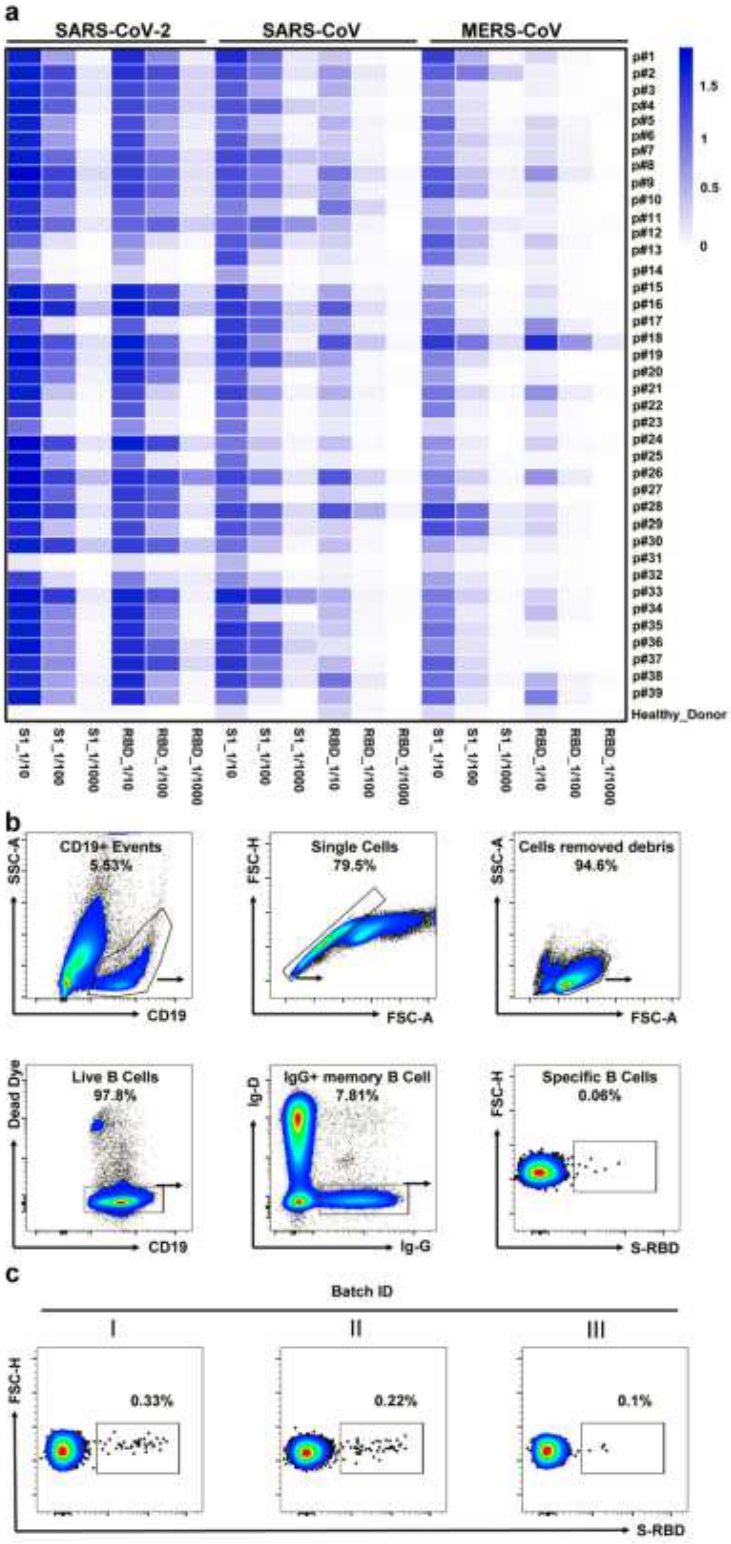

Figure 2

Analyses of plasma response to SARS-CoV-2 and the RBD-specific memory B cells. a The heatmap depicts the specificity of convalescent patients' plasma against S1 or RBD of SARS-CoV-2, SARS-CoV, and MERS-CoV, with serial dilutions, measured by ELISA. The plasma of healthy donors was used as a negative control. Data were shown with the mean of representative experiments. b Gating strategy for SARS-CoV-2 RBD-specific IgG+ mB cells in the PBMC of COVID-19 convalescent patients. Living

CD19+IgD-IgG+ cells were gated, and B cells binding SARS-CoV-2 RBD were selected for single-cell sorting. c FACS analysis of RBD-specific memory B cells in CD19+IgD-IgG+ mB cells from the PBMC of three batches of convalescent patient samples. Plots show CD19+IgD-IgG+ populations using the gating strategy described in b.

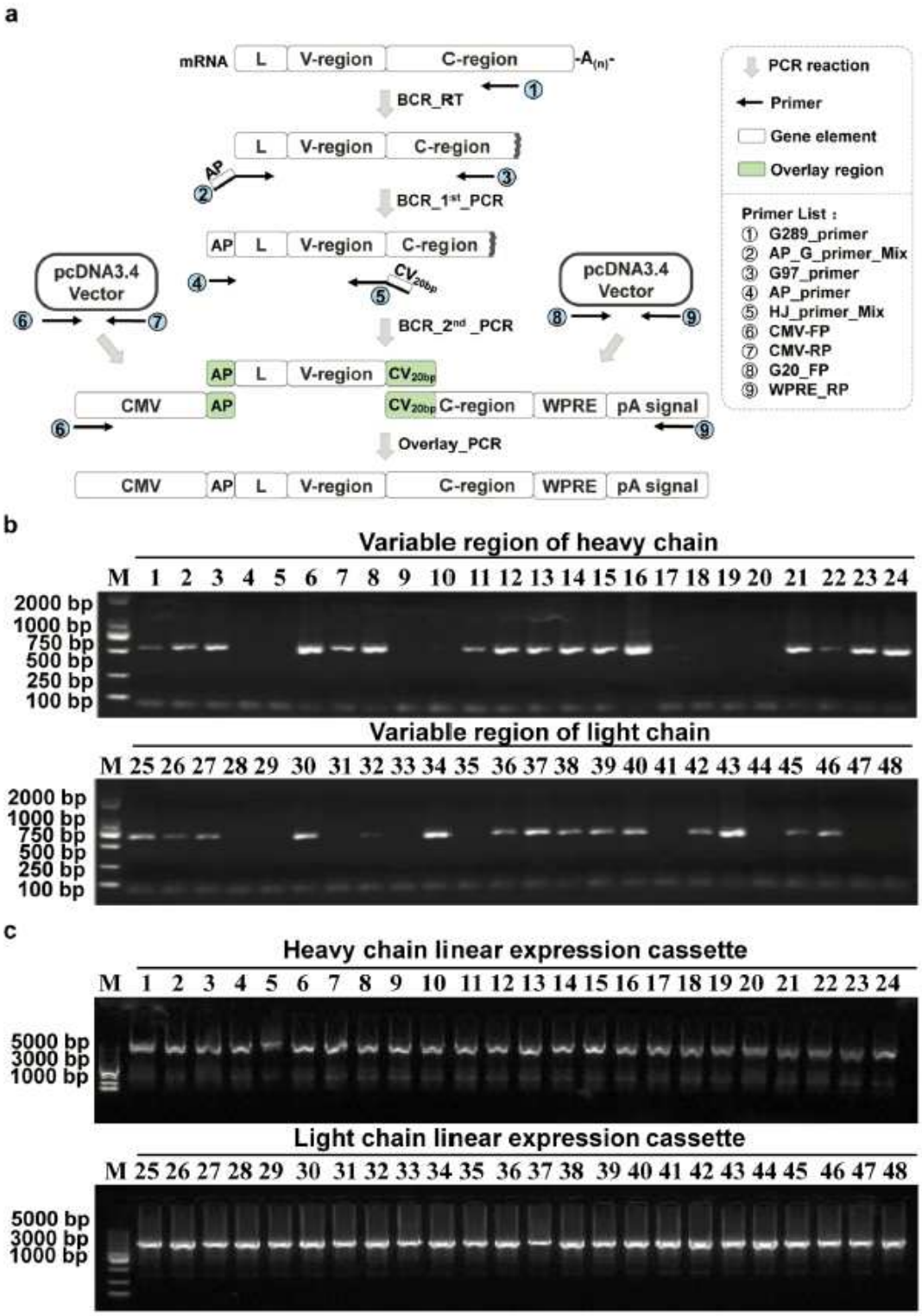

Figure 3

Schematic diagram of the single-cell BCR Cloning and the construction of linear expression cassettes. a The workflow of single-cell BCR Cloning and construction of linear expression cassettes. The BCR cDNAs were obtained from the single RBD-specific mB cells by RT-PCR. the variable region of the Ab gene was amplified via the 1st and 2nd PCR, and the linear expression cassettes were constructed via the 3rd overlay PCR. 1st PCR utilized gene-specific primers at both the 5' and 3' ends. The 5' forward primer including an "adapter" bound to the leader sequence of Ab cDNA (L). The 3' reverse primer bound to the heavy or light constant regions. In the 2nd PCR, the 5' forward primer annealed to an "adapter" locating at the 5' end of the 1st PCR product, and the 3' reverse primer annealed to the J gene of the Ab variable region. The 2nd PCR product provided 20

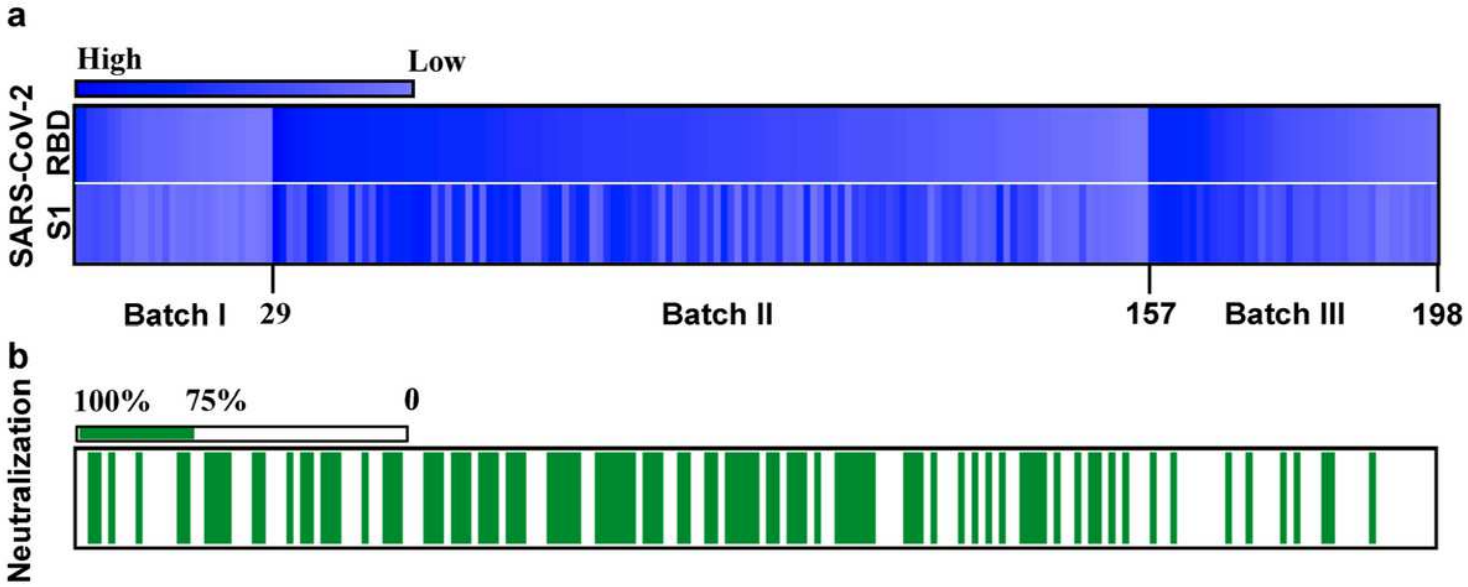

Figure 4

Identification of RBD neutralizing antibodies from convalescent COVID-19 patients. a Screening of SARS-CoV-2 RBD-specific Abs. Antibodies were expressed in HEK293T cells by transfection of the linear Ab expression cassettes. Two days later, antigen reactivity of supernatants to SARS-CoV-2 S subunit S1 or RBD were tested by ELISA. The heatmap reveals that the binding ability of 198 supernatants. The brightness of blue represented the binding strength, which was reflected by the OD405 nm value. The mAbs were ranked by the order of the antigen reactivity screening. b Screening of the potential NAbs. the neutralizing capability were identified by SARS-CoV-2 pseudovirus neutralization assay. The Green columns indicate potential neutralizing Abs (inhibition >75%), while white indicate partial or not neutralizing Abs (inhibition < 75%). The mAbs were ranked as same as the above screening order.

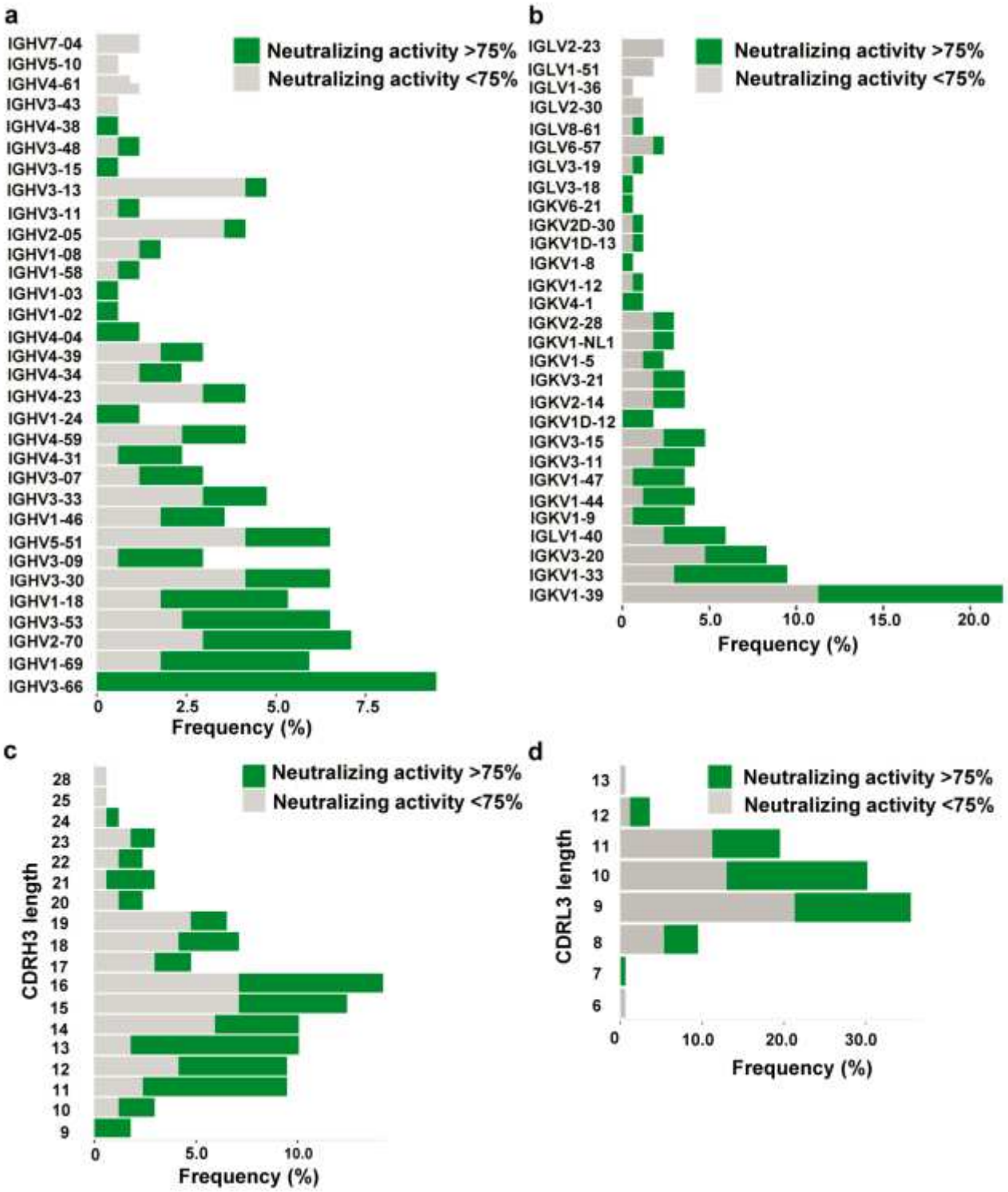

Figure 5

Usage frequencies of the variable region gene clusters and the CDR3 lengths. a Usage frequencies of the variable region gene clusters of the heavy chain (VH) for the pote-NAbs and non-neutralizing Abs. 158 unique Abs sequences were used for calculating of gene frequency. b Usage frequencies of the variable region gene clusters of the light chain (VL) for the pote-NAbs and non-neutralizing Abs. c Frequencies of the heavy chain complementarity determining region 3 (CDRH3) lengths of the pote-NAbs and non-

neutralizing Abs. d Frequencies of the light chain complementarity determining region 3 (CDRL3) lengths of the pote-NAbs and non-neutralizing Abs.

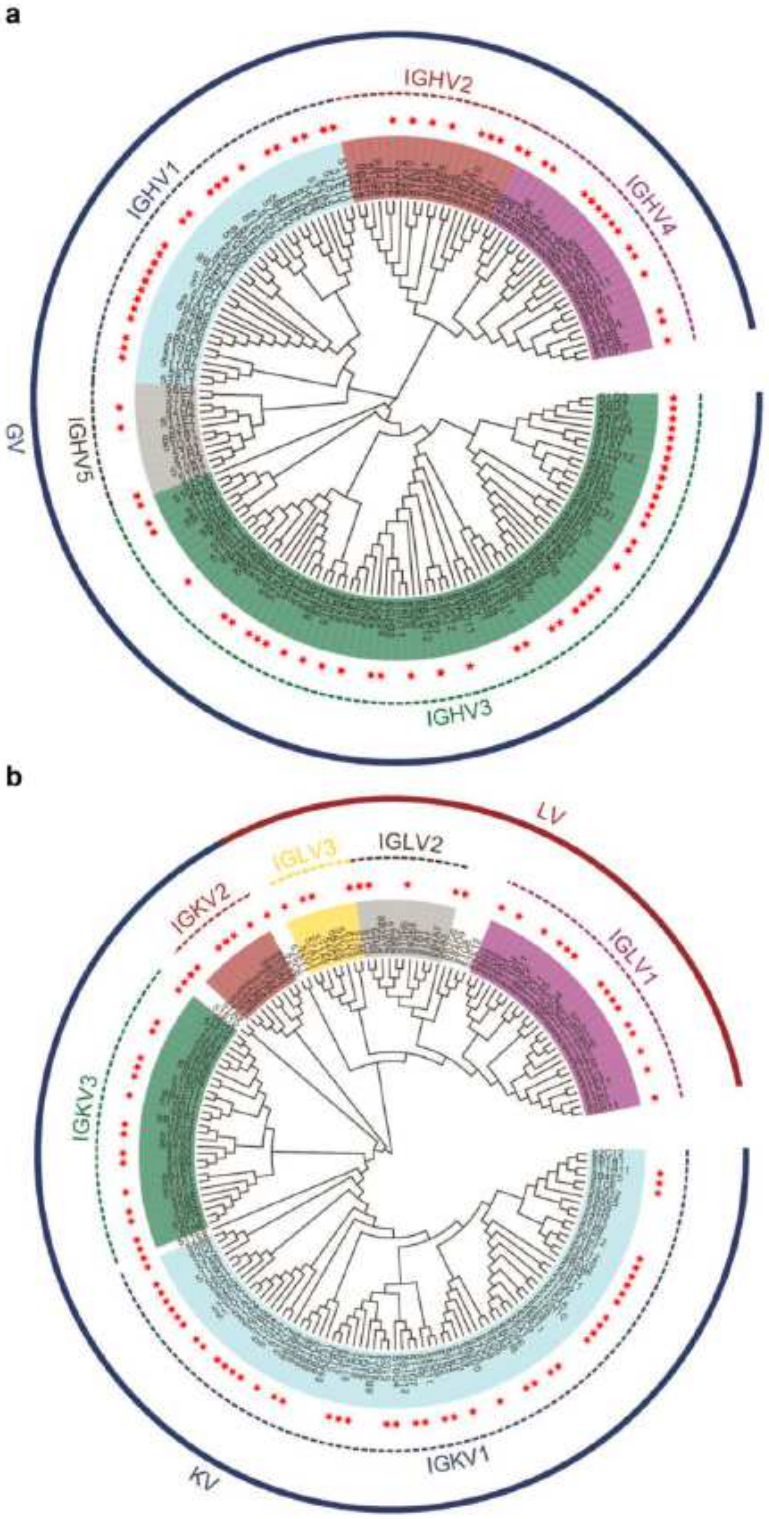

Figure 6

Phylogenetic analysis of variable region genes in the heavy chain (VH) and the light chain (VL) for the RBD-specific mAbs. The red stars represented individual NAbs.

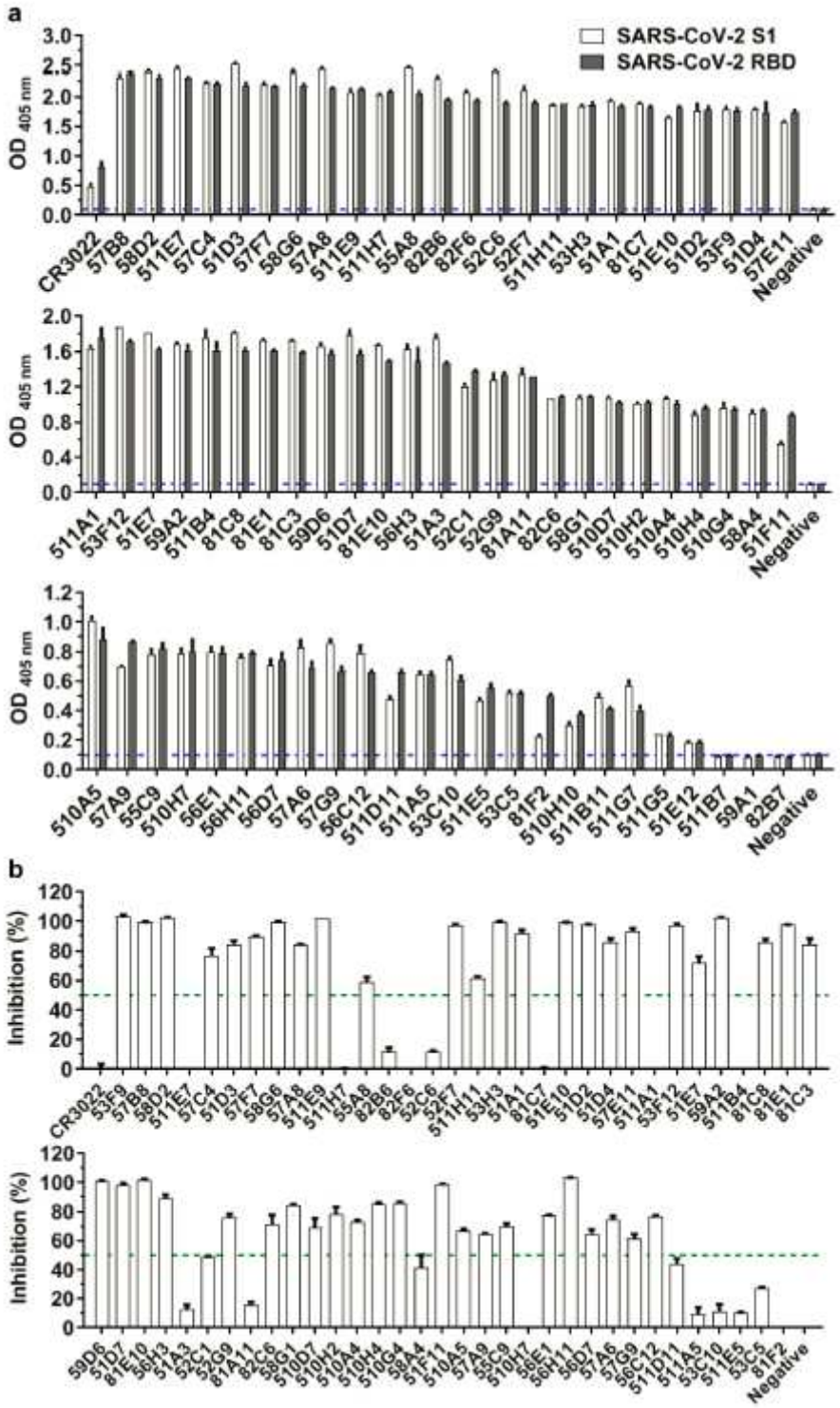

Figure 7

The binding and blockage activity characterizations of mAbs. a The binding strength of purified mAbs. ELISA was used for testing binding strength, and 1 μg/ml SARS-CoV-2 S1 or RBD was coated on the 384 wells plate. The OD405 nm values was measured. A SARS-CoV specific mAb (CR3022) was used as the positive control. The blue dashed lines indicated the OD405nm value of negative interactions. b The inhibitory effect of purified mAbs against the interaction between SARS-CoV-2 RBD and ACE2, tested via

competitive ELISA analysis. The green dashed lines indicated a 50% inhibition on blocking the ACE2-RBD interaction. Data were shown as mean ± SD of representative experiments.

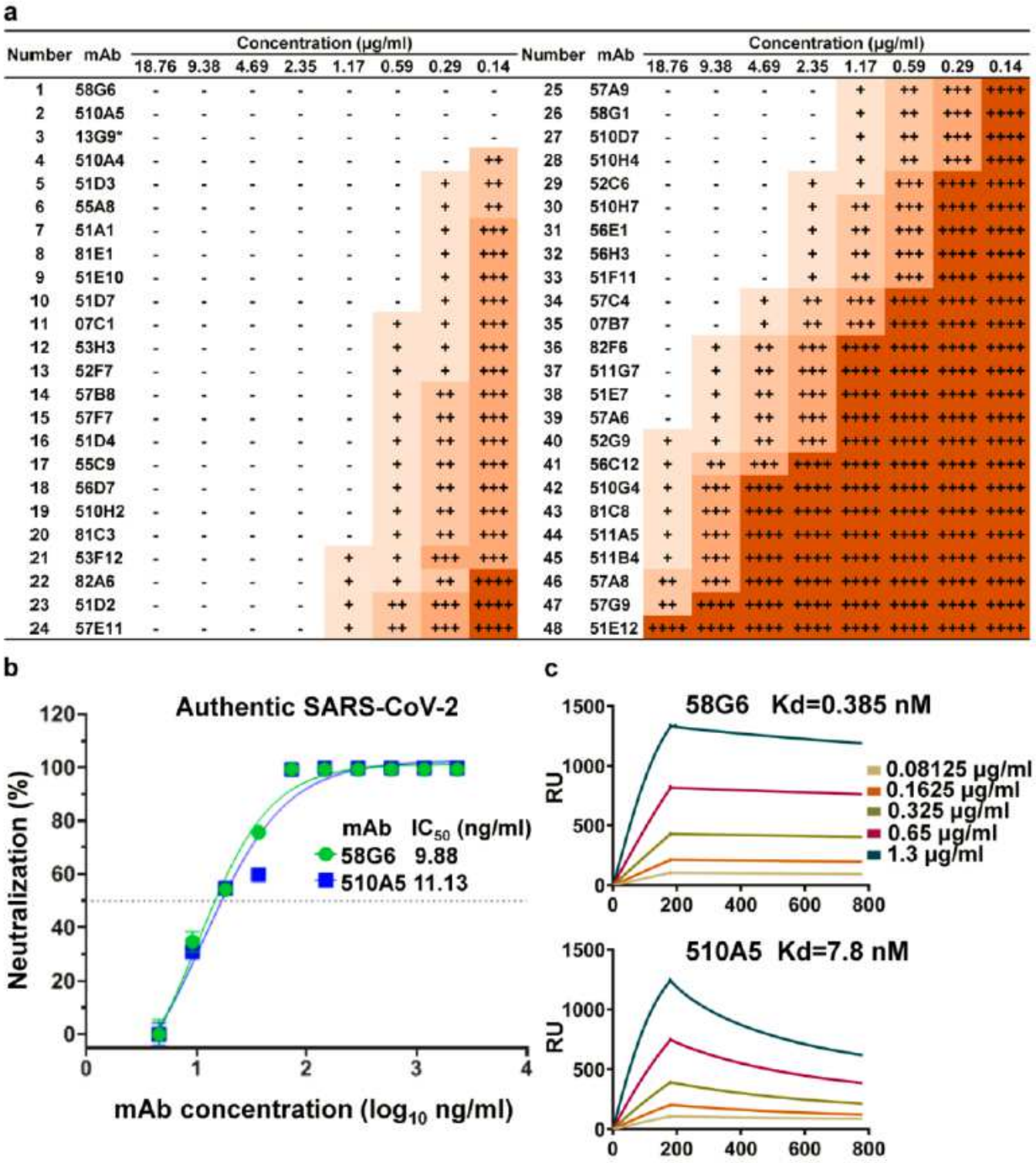

Figure 8

Functional characterization of NAbs against authentic SARS-CoV-2. a The neutralization activities of mAbs against authentic SARS-CoV-2 virus (nCoV-SH01), analyzed by the Cytopathic effects (CPE) test. Serial dilutions of each mAbs were tested, ranging from 18.76 μg/ml to 0.14 μg/ml. CPE results was

summarized in (A), where "++++" indicates 100% cytopathy, "+++" indicates 50-75% cytopathy, "++" indicates 25-50% cytopathy, "+" indicates <25% cytopathy and "-" indicates no cytopathy. 13G9 was marked with "*" to indicate that it was obtained by the method previously described30. b IC50 of 58G6 and 510A5 against the authentic SARS-CoV-2 virus, determined in Vero-E6 cells by RT-qPCR. Dashed lines indicated a 50% inhibition rate of viral infection. Data were shown as mean ± SD of representative experiments. c Binding kinetics of 58G6 (top) and 510A5 (bottom) to SARS-CoV-2 RBD, measured by Surface Plasmon Resonance (SPR). The purified mAbs was captured onto the CM5 sensor chip coating with anti-human IgG-Fc Ab, followed by the injection of soluble SARS-CoV-2 RBD at five different concentrations. The x-axis represents seconds. The results are representatives of two independent experiments.

Supplementary Files

This is a list of supplementary files associated with this preprint. Click to download.

- SupplementaryMaterials.pdf
- SourceDataFig.2a.xlsx
- SourceDataFig.4.xlsx
- SourceDataFig.5.xlsx
- SourceDataFig.7.xlsx
- SourceDataFig.8.xlsx